OPTIMAL DESIGN OF A BIOGAS POWERED $LiBr$-H_2O VAPOUR ABSORPTION SYSTEM

By

MOHD. ALTAMUSH SIDDIQUI

DEPARTMENT OF MECHANICAL ENGINEERING
INDIAN INSTITUTE OF TECHNOLOGY KANPUR

FEBRUARY, 1985

OPTIMAL DESIGN OF A BIOGAS POWERED $LiBr\text{-}H_2O$ VAPOUR ABSORPTION SYSTEM

A Thesis Submitted
in Partial Fulfilment of the Requirements
for the Degree of

MASTER OF TECHNOLOGY

By

MOHD. ALTAMUSH SIDDIQUI

to the

DEPARTMENT OF MECHANICAL ENGINEERING
INDIAN INSTITUTE OF TECHNOLOGY KANPUR

FEBRUARY, 1985

CERTIFICATE

This is to certify that the thesis entitled "Optimal Design of a Biogas Powered LiBr-H_2O Vapour Absorption System" by Mohd. Altamush Siddiqui is a record of work carried out under our supervision and has not been submitted elsewhere for a degree.

B. Sahay
Professor
Dept. of Mechanical Engg.
Indian Institute of Tech.
Kanpur-208016

Manohar Prasad
Assistant Professor
Dept. of Mechanical Engg.
Indian Institute of Tech.
Kanpur-208016

February, 1985

ACKNOWLEDGEMENT

I express my whole hearted gratitude to Dr. Manohar Prasad and Dr. B. Sahay for their valuable guidance and critical appraisal throughout the work. Their constant inspiration and encouragement helped in carrying out the experimental setup.

Thanks to Dr. D.P. Rao (Chemical Engg. Department) and Dr. K.K. Saxena (Mechanical Engg. Department) for their suggestions in the design of the components and the experimental setup of the system.

Thanks to Mr. P.N. Misra for his assistance in the assembly of the system. Thanks to the technical staffs of the Central Workshop, TA 203 Lab. and Glass Blowing, etc. Thanks to Mr. Sharma and his staff for their patience in fabricating the glass instruments for the measurement of pressure, temperature, etc.

Thanks to all my friends and well wishers for their kind help.

Thanks to Mr. D.P. Saini and Mr. Ayodhya Prasad for their patience in typing and Cyclostyling.

MOHD. ALTAMUSH SIDDIQUI

CONTENTS

LIST OF FIGURES

NOMENCLATURES

A	:	cross-sectional area, m^2
A_f	:	fin surface area, m^2
A_o	:	outer cross sectional area, m^2
A_i	:	inner cross sectional area, m^2
C_1	:	capital cost of biogas plant, Rupees
C_2	:	yearly cost of biogas plant, Rupees/year
C_T	:	total yearly running cost of biogas plant, Rupees/year
C_p	:	specific heat, kJ/kg-°C
C_{pw}	:	specific heat of water, kJ/kg-°C
C_{p_L}	:	specific heat of LiBr-H_2O, solution, kJ/kg-°C
C_{s_f}	:	constant described by the liqd. surface combination
COP	:	coeff. of performance of refrigerating system
d	:	tube diameter, m
D	:	Pipe, cylinder diameter, m
D_b	:	bubble diameter, m (defined by Eq. 4.35)
FF	:	finning factor, defined by Eq. (4.9)
F_{1-2}	:	shape factor from body 1 to body 2
G	:	mass flux, kg/m^2-h
h	:	heat transfer coefficient, kJ/m^2-h-°C
h_{lv}	:	latent heat of vaporization/condensation

h'_{lv} : effective latent heat of vaporization/condensation allowing for the effect of superheat, kJ/m^2-h-°C

h_{red} : reduced heat transfer coefficient defined by Eq. (4.10)

h_i : inside heat transfer coeff. kJ/m^2-h-°C

h_o : outside heat transfer coeff. kJ/m^2-h-°C

h_f : fin side heat transfer coeff. kJ/m^2-h-°C

h_{r_g} : radiative heat transfer coeff. in the generator, kJ/m^2-h-°C

h_r : energy release due to respiration per tonne mass per unit time

h_c : convective heat transfer coefficient kJ/m^2-h-°C

k : thermal conductivity, kJ/m-h-°C

$\bar{l}'$: characteristic lengthfor fin, m

L_{suffix} : length of tubing, piping of the respective system components, m

L : life of the biogas plant, years

m : mass flow at any section per unit mass flow through evaporator (kg/kg)

$\dot{m}$: mass flow rate, kg/h (suffixes indicate the state points)

n : number of fins per meter length

q : heat transfer rate per unit length of the tube, kJ/h

$\dot{Q}$: heat transfer rate per TR, kJ/h

Q : total heat transfer rate, kJ/h

Q'_g : heat load on the generator, kJ/day

Q_{gas} : heat abstracted from the biogas, kJ/m^3

r	:	radius of circular fin equivalent to square fin, m
r_i , r_o	:	inside and outside radius of tube, m
r^*	:	dimensionless parameter, $(\frac{r + \delta/2}{r_o})$
T	:	temperature, °C
T_{am}	:	maximum ambient temp. (= 41.3°C for Kanpur city)
ΔT_m	:	LMTD, log mean temperature difference, °C
TR	:	tonnage of refrigeration
U_o	:	overall heat transfer coeff., unfinned, kJ/m^2-h-°C
U_{f_o}	:	overall heat transfer coeff., finned, kJ/m^2-h-°C
V	:	volume of biogas, m^3/day
x	:	concentration of LiBr in water, percent
$\bar{x}$	:	quality of water vapour

<u>Non-dimensional Parameter</u>

Gr	:	Grash of number, $\frac{\bar{l}^3 \rho^2 \ \beta \ g. \ T}{\mu^2}$ or $\frac{d^3 \rho^2 \ \beta \ \ T}{\mu^2}$
Gz	:	Graezt number, Re Pr (d/L)
Pr	:	Prandtle number, $C_p \ \mu/k$
Re	:	Reynolds number, d G/μ
Nu	:	Nusselt number, $\frac{hd}{k}$ or $\frac{hl}{k}$

GREEK LETTERS

δ	:	Fin thickness, m
δ'	:	Wall thickness (in the conduction of heat from inner to outer surface), m
Ψ	:	Parameter defined: $\overline{1\sqrt{h/k(\delta/2)}}$
ϕ	:	Fin effectiveness
σ	:	Stephan Boltzman constant = $20.42\times10^{-8}\ \frac{kJ}{m^2\text{-}h\text{-}K^4}$
ε_r	:	emmissivity, 1.0 for a black surface
μ	:	dynamic viscosity, kg/m-h
ρ	:	density, kg/m^3
ΔT	:	temperature difference, °C
β	:	coefficient of thermal expansion, 1/T, (1/K)
ν	:	kinematic viscosity, (μ/ρ), m^2/h
°C	:	degree Celcius
K	:	degree Kelvin
σ_t	:	surface tension, N/m
ϵ_1, ϵ_2	:	precooler and preheater effectivenesses, respectively $(\epsilon = \epsilon_1 = \epsilon_2)$

SUBSCRIPTS

a	:	absorber side
c	:	condenser side
e	:	evaporator side
f	:	fin
g	:	generator side
go	:	optimum generator
i	:	inside
l	:	liquid
o	:	outside
r	:	radiative
s	:	saturated
sp	:	superheat
v	:	vapour
w	:	wall
x	:	helix

ABSTRACT

A pumpless LiBr-H_2O vapour absorption system has been designed to operate using biogas as a source of energy. The capacity of the system is selected on the basis of the requirement of an average agricultural family. Optimum generator temperatures for different operating conditions have been obtained based on economic criteria and are shown graphically. The design of the system components is done for the optimum generator temperature corresponding to the generator pressure of 80 mm of mercury and the evaporator temperature of 5°C. The conditioned space can be maintained at about 7 to 8°C. The heat rejection from the system is by natural convection of air. The temperature difference between the maximum ambient temperature and the designed condition for heat rejection to the former is about 5 to 6°C.

The present work would be most helpful in the design of a refrigerator, water cooler or an air-conditioner for different operating conditions. The system designed would serve the agrobased rural community in preserving eatables, vaccines, vital medicines, etc.

The effects of effectivenesses on biogas cost have been studied. The variation in biogas cost with system capacity has been also studied. Multipliers were computed for evaporator temperatures other than 5°C such that the same would enable the users to utilize the present results for a wide range of operation.

Components of the refrigeration system have also been fabricated and assembled. In the limited time inspite of best efforts, it was not possible to make the assembly completely leakage-free, which is essential for sustained running of the set-up and experimentation.

The detailed method for the design of various components would enable users to design the system components to suit their requirement.

CHAPTER - I

INTRODUCTION

1.1 Social Rammifications

The attractive city life and poor village management is causing heavy influx of people from rural areas to cities. This is posing threat to appropriate urban life and is becoming totally beyond the manageable limit of various authorities. As such if the living standard and job opportunities (need of the day in the national interest) are improved in the rural areas, there will be tremendous reduction in the rural outflux to cities. The reduction in influx to city would also reduce traffic load and urban housing shortage.

1.2 Energy Demand

Presently, the escalating cost of energy and impending fuel shortages have created interest in the research and development of alternate energy resources. A few such promising sources which have been under active investigation and development [1,2,3,4,5], are the solar energy, biomass energy, wind energy, tidal energy, waste heat recovery, etc.

1.3 Rural Applications

A wide spectrum of work is being done in the field of solar energy. Thus solar powered cookers, heaters, refrigerators, air conditioners, etc. are gaining market day by day. The biomass energy is a good source specially for agrobased rural areas and at places where electricity failure is frequent. Our country is an agricultural land and the cultivation is mostly done using oxen, and for milk buffaloes and cows are tamed. It means the availability of animal dung is a continuous and everlasting source. If biogas is produced from the dung, it would provide better rural life. The fermentation increases manure value of animal dung by as high as 40% [6]. This would cause considerable curtailment in synthetic fertilizer. Moreover the use of natural fertilizer retains better productivity of land. Also, the extraction of the biomass energy, which is mostly from the organic materials, being wasted, solve the problem of pollution. Use of biogas also reduces demand for wood etc. as cooking fuel, which saves the trees from being cut in large scale. Biogas has been widely used for cooking and lighting. The hybridization of biogas has been proposed in [7] to serve as a standby power source for the solar powered vapour-absorption refrigeration system. A family may need a 0.1 ton capacity refrigerator operating for about 12 hours

per day (at generator pressure, p_g = 80 mm of H_g, evaporating temperature, T_e = 5°C with COP = 0.746) using 1.32 m^3/day of gobar gas. For a normal family, cooking gas required/day is 1.4 m^3/day and for lighting is 1.2 m^3/day. Thus, total gas required turns out to be approximately 4 m^3/day. An average animal dung (wet) yield [8] is about 15 kg/day, giving about 0.04 m^3 of biogas per kg of dung, requiring about 6 to 7 animals, which is normally within the scope of a good agricultural family.

1.4 The Refrigeration System

The vapour-absorption system eliminates the tremendously large compression energy, owing to the reason that the system operates at low pressures, requiring negligible pumping energy. The special feature of the vapour-absorption is the use of thermal energy, a low grade energy as a byproduct of waste heat from the process industry, blast furnace, steel plants, automobile exhausts, solar energy or biogas energy. Further, its COP can be kept high even if the evaporator temperature falls. A comparative study [9] for a single stage refrigerant absorbent combination is given in table 1.1.

Table 1.1

Comparative study of various refrigerant-absorbent combinations [9]

Absorbent-refrigerant combination	NH_3-H_2O	NH_3-$LiNO_3$	NH_3-NaSCN	Sink Temperature T_c = 30°C
Generator temperagure T_g, °C	115 140	90 115	100	
Evaporating temperature, T_e, °C	-10 -25	-10 -25	-10	

Available fluid temperature from the flat plate collector [9] covers a range from approximately 80°-115°C, but are generally below 90°C. It can be used to run systems for which generation temperature is not large. Also waste heat available is at a temperature of about 100°C.

It has been reported [10,11,12] that LiBr-H_2O is the best combination for the optimum performance of vapour-absorption system temperature above 4°C. The COP of this system varies from 0.6 to 0.75, whereas, the COP of NH_3-NaSCN and NH_3-H_2O systems vary from 0.11 to 0.27 and 0.05 to 0.14, respectively.

1.5 Economic Factors

The limitation in the availability of the temperature from the solar collectors necessitates the use of

other sources yielding higher temperatures. Biogas is one workable at a wide range of temperatures; limit being put to the available capacities of biogas plants. In India biogas units of 2,3,4 and 6 m^3/day have been widely used. Also, the cost comparison between the available energy resources and the renewable ones show that the initial investment is quite high, but in the long run it is comparable with other sources. It is reported in [8] that the energy from 1 m^3 of biogas is equivalent to that of 0.62 litre of kerosene oil and 4 kg of firewood. The cost of 1 m^3 of biogas is estimated to be Re.0.72 per day if the life of biogas plant is taken as 15 years. In the same way the cost of biogas required in the refrigerating unit of 0.1 ton capacity (for 1.32 m^3/day) is about Re.0.84 per day, whereas, cost of electrical power in the vapour-compression system for the same capacity and time of operation is about Re. 0.66 per day (i.e., 0.048 kW x 12 hour x Re. 0.55). For higher capacities the cost of biogas reduces considerably. This comparison, obviously does not have any meaning where electricity is rarely available or not available at all.

1.6 Present Work

The objective of the present work is to develop a cooling unit which would preserve eatables at about 7 to 8 °C especially for the agrobased areas using biogas

as a source of energy. With this view economic cost analysis of the biogas required in the generator of the LiBr-H_2O vapour-absorption system has been done at various operating conditions, and the optimum generator temperatures have been evaluated correspondly. The optimization has been carried out for NH_3-H_2O combination using flat plate collector as a source of energy [13]. LiBr-H_2O system using solar energy has been optimized with respect to maximum COP [7]. It reports for p_g = 71.9 mm of H_g and T_e = 5°C, optimum generator temperature, T_{g_o} = 93°C (using precooler and preheater both, ε = 0.8) and T_{g_o} = 103.5°C (for ε = 0). In the present work of optimization, the generator temperature T_g is varied keeping the generator pressure p_g, the evaporator temperature T_e and precooler and preheater effectivenesses as parameters. The COP and the available energy to the generator, Q_{gas} are functionally related to T_g. The yearly running cost and the capital cost for biogas plant are functionally related to T_g using least square regression technique. Results are obtained for different refrigeration capacities as well.

The components of the refrigerating system have been designed on the basis of optimum values obtained at generator pressure 80 mm of H_g, T_e = 5°C and ε_2 = 0.75 (only preheater is used). In the fabrication and assembly

of such a system having large number components, even slightest leakage hampers the experiment because of the vacuum (1 atm) to be maintained inside the system tubings. To realize a completely leakage free set-up, it normally requires considerable amount of time. The system has been fabricated and instrumented, but very minute leakages still remain to be rectified in order to obtain reliable experimental data.

CHAPTER - II

MATHEMATICAL FORMULATION

2.1 System Selection

Since the aim is to develop a cabinet refrigerator or a cooling unit required in primary health care centres mainly for the agrobased areas, it is necessary that the system be simple, cheap and independent of electricity. The most common absorption refrigeration systems are NH_3-H_2O , LiBr-H_2O, NH_3-NaSCN and NH_3-$LiNO_3$. Comparative study among these show [10,11,12] that LiBr-H_2O absorption system would be the best amongst all. In this system water acts as a refrigerant and Lithium bromide (salt) as an absorbent. Few attractive features of LiBr-H_2O system are presented below:

a) Higher COP values, about 0.6 to 0.75.

b) Pure water vapour leaves the generator since LiBr does not evaporate. Hence an analyzer and a rectifier are eliminated giving a simple system.

c) Purging of water from the evaporator is trivially eliminated.

d) Overall working pressure in the system is barely above 0.15 bar (100 mm of H_g absolute), there is no need to design the system along high pressure codes.

e) The pressure inside the system is below atmosphere, hence no fear of bursting or accidental hazard.

f) Water being non-toxic and nonflammable, the system can be used directly for chilling coil for the air conditioners.

g) Since the difference in the operating pressures between the generator and the evaporator is very small, the pumping energy required is negligible. Moreover, pumping mechanism is eliminated simply by the adjustment of the elevation by a metre or so of the absorber, generator and the evaporator; whereas, the elevation has to be increased by 100 metres to achieve the operating pressure difference in NH_3-H_2O system. Thus, LiBr-water system is free from vibration and noise as well. Hence no strong foundation required.

h) No leakage in the system, since shaft seal is absent.

i) Cost of the system is very small since there are no moving parts, glands, valves, etc.

j) No electrical energy required.

k) Water having higher enthalpy of vaporization than

NH_3 is used. The refrigerant is almost free of cost. With these advantages the $LiBr-H_2O$ system is selected for the present work.

2.2 System Description

Absorption cycles are heat operated in which a secondary fluid, the absorbent, absorbs the primary fluid, gaseous refrigerant from the evaporator maintained at low pressure. Absorption takes place because of more affinity of absorbent for the refrigerant. To augment the absorption in small volume of absorber, the large contact area is provided. The energy released [14] during the absorption process is due to heat of condensation, sensible heat and heat of dilution, which is rejected to a sink.

The refrigerant-absorbent solution is pumped into the generator via a heat exchanger where the refrigerant and the absorbent are separated by a distillation process, because at higher temperature the absorbent has less affinity for the refrigerant molecules. If the pure absorbent is non-volatile, as in $LiBr-H_2O$ system, a simple still is adequate. But in systems using volatile absorbents, like water in NH_3-H_2O , would require additional distillation equipments such as analyzer and rectifier. If the refrigerant is not essentially free of absorbent,

vaporization in the evaporator is hampered. If the absorbent material tends to become solid, as in $LiBr-H_2O$ system, enough refrigerant must be present to keep the pure absorbent material in the dissolved form at all times; and can be checked by avoiding excessive heating in the generator.

Figure 2.1(a) exhibits the vapour-absorption system having different components. The cycle with state points is shown in Fig. 2.1(b). The weak solution of $LiBr-H_2O$ from absorber is pumped into the generator through a preheater (PH) in order to reduce heat transfer, Q_g, to the generator. The strong solution returns to A through the preheater and throttle valve. The refrigerant vapour from the generator is condensed in C and then throttled to the evaporator E. The condensate gets subcooled in the precooler (PC) by the evaporator vapour. Thus, the refrigeration effect gets enhanced. The refrigeration effect Q_e is produced in the evaporator due to vaporization of water.

2.3 Mathematical Modelling

2.3.1 Thermodynamic analysis of the system

Absorber:

Referring to Fig. 2.1(a), the mass conservation in terms of concentration of the absorbent across absorber is given by:

$$m_6\, x_6 + m_7\, x_7 = m_1\, x_1 \qquad (2.1)$$

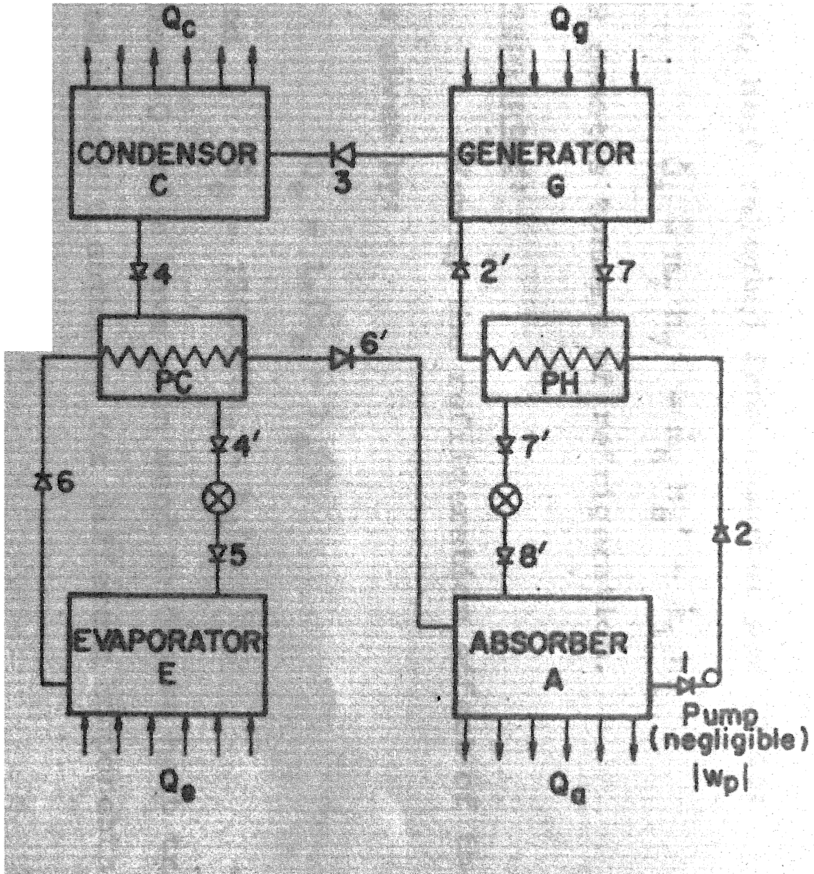

Fig.2.1(a) LiBr-water vapour absorption system.

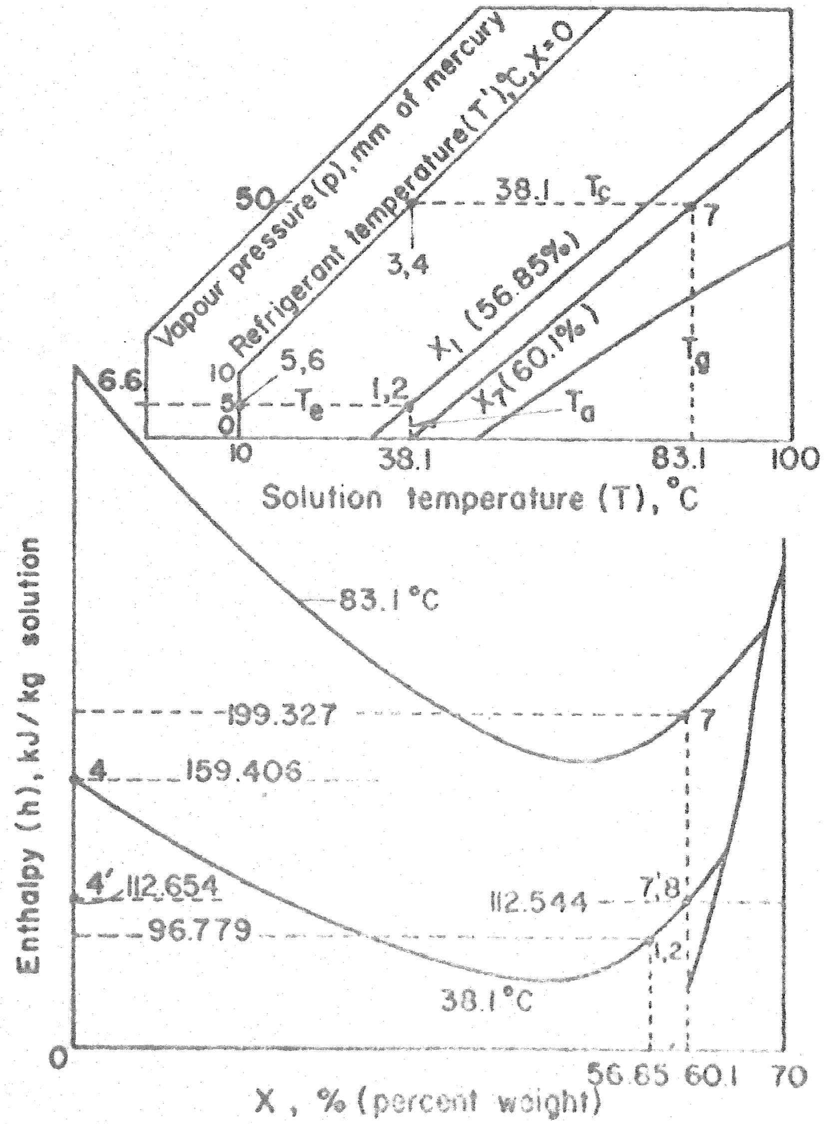

Fig.2.1(b) Lithium Bromide Concentration (X)

where m and x denote for mass and concentration, respectively at different state points.

Since the pure vapour flows out of the evaporator, $x_6 = 0$. With $m_6 = 1$ and $m_7 = m_1 - 1$. One gets from Eq. (2.1) as:

$$m_1 = x_7/(x_7 - x_1) \tag{2.2}$$

and

$$m_7 = x_1/(x_7 - x_1) \tag{2.3}$$

Also,

$$\dot{m}_1 = \dot{m}_6 \cdot m_1 \tag{2.4}$$

$$\dot{m}_7 = \dot{m}_6 \cdot m_7 \tag{2.5}$$

where $\dot{m}_6$ is defined by Eq. (2.8).

Now, heat rejected from absorber per TR is:

$$\dot{Q}_a = \dot{m}_7 h_7' + \dot{m}_6 h_6' - \dot{m}_1 h_1 \tag{2.6}$$

TR denotes tonnage of refrigeration.

<u>Evaporator</u>:

Hence, the refrigeration effect of the system is given by:

$$Q_e = 1.(h_6 - h_4') \tag{2.7}$$

and

$$\dot{m}_6 = 12600/(h_6 - h_4') \tag{2.8}$$

where Q and h have been used to denote heat transfer and specific enthalpy for different components and state points, respectively.

Generator:

Energy balance for the generator gives:

$$Q_g = m_3 h_3 + m_7 h_7 - m_2' h_2' \qquad (2.9)$$

Using: $m_3 = m_4 = m_4' = m_5 = m_6 = m_6' = 1$ kg

$m_1 = m_2 = m_2'$; $m_7 = m_7' = m_8$

One gets :

$$Q_g = [h_3 + (x_1 h_7 - x_7 h_2')/(x_7 - x_1)] \qquad (2.10)$$

Heat load in the generator per TR is :

$$\dot{Q}_g = \dot{m}_3 \cdot Q_g \qquad (2.11)$$

where $\dot{m}_3 = \dot{m}_6$

Precooler:

The enthalpy of subcooled condensate, h_4' is:

$$h_4' = h_4 - \varepsilon_1 (h_6' - h_6) \qquad (2.12)$$

where ε_1 is effectiveness of the precooler.

Preheater:

Similarly, for the preheater (effectiveness, ϵ_2):

$$h_2' = h_1 + \varepsilon_2 (x_1/x_7) (h_7 - h_7') \qquad (2.13)$$

Hence,

$$COP = Q_e/Q_g = (h_6 - h_4')/[h_3 + (x_1 h_7 - x_7 h_2')/(x_7 - x_1)] \ldots. (2.14)$$

Condenser:

Heat rejection from the condenser per TR is:

$$\dot{Q}_c = \dot{m}_3 \; (h_3 - h_4) \qquad (2.15)$$

The thermodynamic properties of LiBr-H_2O solution of [15] have some inconsistency. The proper units have been taken from [14], which are in terms of operating temperature, pressure and concentration of the solution, given in Appendix A. Also, the properties of pure water [16] are listed in A. The calculations are made in S.I. units.

2.3.2 Functional Relation for COP [13]

Using appropriate equations and properties, COP's were computed at different generator temperatures for a set of operating parameters such as the generator pressure being equal to that of condenser, the evaporator temperature and precooler and preheater effectiveness. Thereafter COP's were functionally related to T_g using least square error regression method for each set.

$$\text{i.e.,} \quad COP = \sum_{j=0}^{j=9} a_j \, T_g^j = F_1(T) \qquad (2.16)$$

2.3.3 Useful Energy from Biogas

Composition of the biogas was taken as [3,6]:

$$\text{(Methane) } CH_4 - 55\% \text{ and (Carbondioxide) } CO_2 - 45\% \qquad \ldots (2.17)$$

Combustion equation can be written as:

$$0.55\ CH_4 + 0.45\ CO_2 + a\ (O_2 + 3.76\ N_2) \rightarrow$$
$$CO_2 + 1.1\ H_2O + bO_2 + 3.76\ a\ N_2 \qquad (2.18)$$

where a and b are constants.

In order to promote better air fuel mixing 10% excess air is used. Hence,

$$\frac{b}{1 + b + 3.76\ a} = 0.1 \text{ or } 0.9\ b = 0.1 + 0.376\ a \qquad \ldots\ldots \quad (2.19)$$

$$O_2 \text{ balance gives:} \quad 0.45 + a = 1 + 0.55 + b \qquad \ldots\ldots \quad (2.20)$$

Solving Eqs. (2.19 and 2.20), we have, a = 2.08015 and b = 0.98015.

Air fuel ratio,

$$A/F = \frac{\text{mass of } (2.08015 \text{ mole of } O_2 + 7.82136 \text{ mole of } N_2)}{\text{mass of } (0.55 \text{ mole of } CH_4 + 0.45 \text{ mole of } CO_2)} \qquad \ldots\ldots \quad (2.21)$$

1 mole of O_2 , N_2 , CH_4 and CO_2 equal to 32, 28, 16 and 44 respectively. Substituting respective values in Eq. (2.21), we have

$$A/F = 9.9847$$

For a combustion reaction occurring at constant pressure in steady flow, the first law of thermodynamics with enthalpy of combustion can be written as [17],

$$Q_{gas} = \Delta H_s - [Q_{prod.} - Q_{react.}] \qquad (2.22)$$

$$Q_{gas} = \Delta H_s - [\sum_p n_p \{\bar{h}_p (T_p) - \bar{h}_p (T_{sd})\}$$

$$- \sum_r n_r \{\bar{h}_p (T_r) - \bar{h}_p (T_{sd})\}] \qquad (2.23)$$

where,

ΔH_s = Enthalpy of combustion.

Q_{gas} = Heat abstracted from the fuel during combustion process.

n_p , n_r = Number of moles of products and reactants, respectively.

$\bar{h}_p$, $\bar{h}_r$ = Specific enthalpies of products and reactants, respectively (kJ/kg- mole)

T_p , T_r = Temperature.

T_{sd} = Standard temperature, usually 25°C (298.15 K)

Since, only CH_4 burns in the biogas, enthalpy of combustion, from table A-7 [17] at T_{sd} = 298.15 K, ΔH_s = - 11,946 x 4.187 kJ/kg. For 55% methane as reactant,

$$\Delta H_s = 4,40,158.375 \text{ kJ/kg-mole}$$

Rewriting Eq. (2.23) for the combustion equation, Eq. (2.18), we have

$$Q_{gas} = \Delta H_s - [(\{\bar{h}_{CO_2} (T_p) - \bar{h}_{CO_2} (T_{sd})\}$$

$$+ 1.1 \times \{\bar{h}_{H_2O} (T_p) - \bar{h}_{H_2O} (T_{sd})\}$$

$$+ 0.98015 \times \{\bar{h}_{O_2} (T_p) - \bar{h}_{O_2} (T_{sd})\}$$

$$+ 7.82136 \times \{\bar{h}_{N_2} (T_p) - \bar{h}_{N_2} (T_{sd})\})$$

Eq. contd.....

$$- (0.55 \times \{\bar{h}_{CH_4}(T_r) - \bar{h}_{CH_4}(T_{sd})\}$$

$$+ 0.45 \times \{\bar{h}_{CO_2}(T_r) - \bar{h}_{CO_2}(T_{sd})\}$$

$$+ 2.08015 \times \{\bar{h}_{O_2}(T_r) - \bar{h}_{O_2}(T_{sd})\}$$

$$+ 7.82136 \times \{\bar{h}_{N_2}(T_r) - \bar{h}_{N_2}(T_{sd})\})] \quad \ldots \quad (2.24)$$

Let us assume that the reactants burn at room temperature (i.e., $T_{am} = T_r = 314.45$ K) and the products leave at 50°C above the generator temperature. Let us assume that the generator is operating at a temperature, $T_g = 116°C$, so that

$$T_p = T_g + 50 = 439.15 \text{ K}$$

Hence, the specific enthalpies of the various compounds at the corresponding temperatures T_p, T_r and T_{sd}, listed in table 2.1, are taken from table A-9 [17].

Table 2.1

Specific Enthalpies kJ/kg-mole of Various Compounds at Typical Value of T_p, T_r, T_{sd}

Temperature(K) / Compound	T_p 439.15	T_r 314.45	T_{sd} 298.15
CO_2	15,059.13	9,934.81	9,379.34
H_2O	14,727.68	-	8,471.37
O_2	2,897.05	9,097.61	8,668.67
N_2	12,813.47	9,102.56	8,678.69
CH_4	-	8,451.46	8,050.49

Substituting the respective values of specific enthalpies from table 2.1 in Eq. (2.24) we have

$$Q_{gas} = 3,95,790.56 \text{ kJ/kg-mole}$$

Using equation of state at normal temperature and pressure

$$p\bar{V} = \bar{R}T \qquad (2.25)$$

with, $p = 1.013 \times 10^5$ N/m^2, $T = 314.45$ K and $\bar{R} = 8.317$ kJ/kg mole K

$$\bar{V} = 25.7 \text{ m}^3\text{/kg-mole}$$

Making use of the specific volume $\bar{V}$,

$$Q_{gas} = 15,400.41 \text{ kJ/m}^3$$

Similarly, values of Q_{gas} were calculated for different operating temperatures and were functionally related to T (= T_g + 50) as:

$$Q_{gas} = 17,560.37152 - 12.64482465\ T - (1.7546455 \times 10^{-3})\ T^2 = F_2(T) \quad \ldots. \qquad (2.26)$$

2.3.4 Biogas Cost with Volume

From [8], the capital cost of biogas plants and their annual expenditure along with the annual income as reported in " An Economic Analysis of a 3m^3 Gas Plant conducted by the Khadi and Village Industries Commission in India (1978)" [18] is estimated and is functionally related to the biogas volume using the least square regression

method. The capital cost includes the total investment on construction of the biogas plant, piping, stove, etc. The interest on the investment is taken as 9% per annum, depriciation on structure, piping and stove as 5% per annum and cost of painting each year is taken as Rs. 50/litre, constitute the annual expenditure. The annual income includes the cost of gas (taken as Rs. 185/m^3) and the selling price of manure is Rs. 44/ton. The cost of gobar is taken as 1.5 times the selling price of manure, which also adds to the annual expenditure. It is reported [8] that 1 m^3 biogas plant requires 25 kg of gobar, and out of 23 ton gobar, 7 ton is composted and 16 ton is refused. (i.e., useful manure). The effective working days for the biogas plant are assumed as 325 days/year. The cost-volume relation is represented as follows:

$$C_1 = B_1 V^{n_1} \tag{2.27}$$

and

$$C_2 = B_2 V^{n_2} \tag{2.28}$$

where,

$$B_1 = 1597.48672, \quad n_1 = 0.706043244 \tag{2.29}$$

$$B_2 = 220.1583947, \quad n_2 = 0.546585428 \tag{2.30}$$

From Eqs. (2.7, 2.8 and 2.14), the heat load on the generator can also be written as:

$$Q_g' = TR \times 12{,}600 \times 24 \,/\, COP \tag{2.31}$$

Hence, volume of the biogas required for a given capacity and COP of a refrigerating system can be found as:

$$V = Q_g'/Q_{gas} = TR \times 12600 \times 24 \,/\, (COP \times Q_{gas}) \quad \ldots \quad (2.32)$$

Assuming an operating condition of 70% , we have from Eqs. (2.16, 2.26 and 2.32),

$$V = TR \times 12600 \times 24 \times 0.7 \,/\, (F_1(T) \times F_2(T))$$
$$= 211680 \times TR \,/\, F(T) \quad \ldots \quad (2.33)$$

where, $F(T) = F_1(T) \times F_2(T) \quad \ldots \quad (2.34)$

2.4 Optimization

The total cost of the whole system is the objective function related to generator temperature for a set of parameters. The generator temperature should be such that the cost of biogas energy required to operate it is minimum. From Eqs. (2.27 and 2.28) cost of biogas is directly proportional to its volume. Hence, for minimum cost the minimum volume of biogas should be used. From Eq. (2.34) volume of biogas required is minimum if F(T) is maximum, that is, the product of COP and Q_{gas} is maximum. The variation in COP of the system for different pressures along with Q_{gas} with generator temperature is shown in Fig. (2.2).

If C_2 exists at the end of each year of L years and R is the interest rate, the present worth, P is obtained

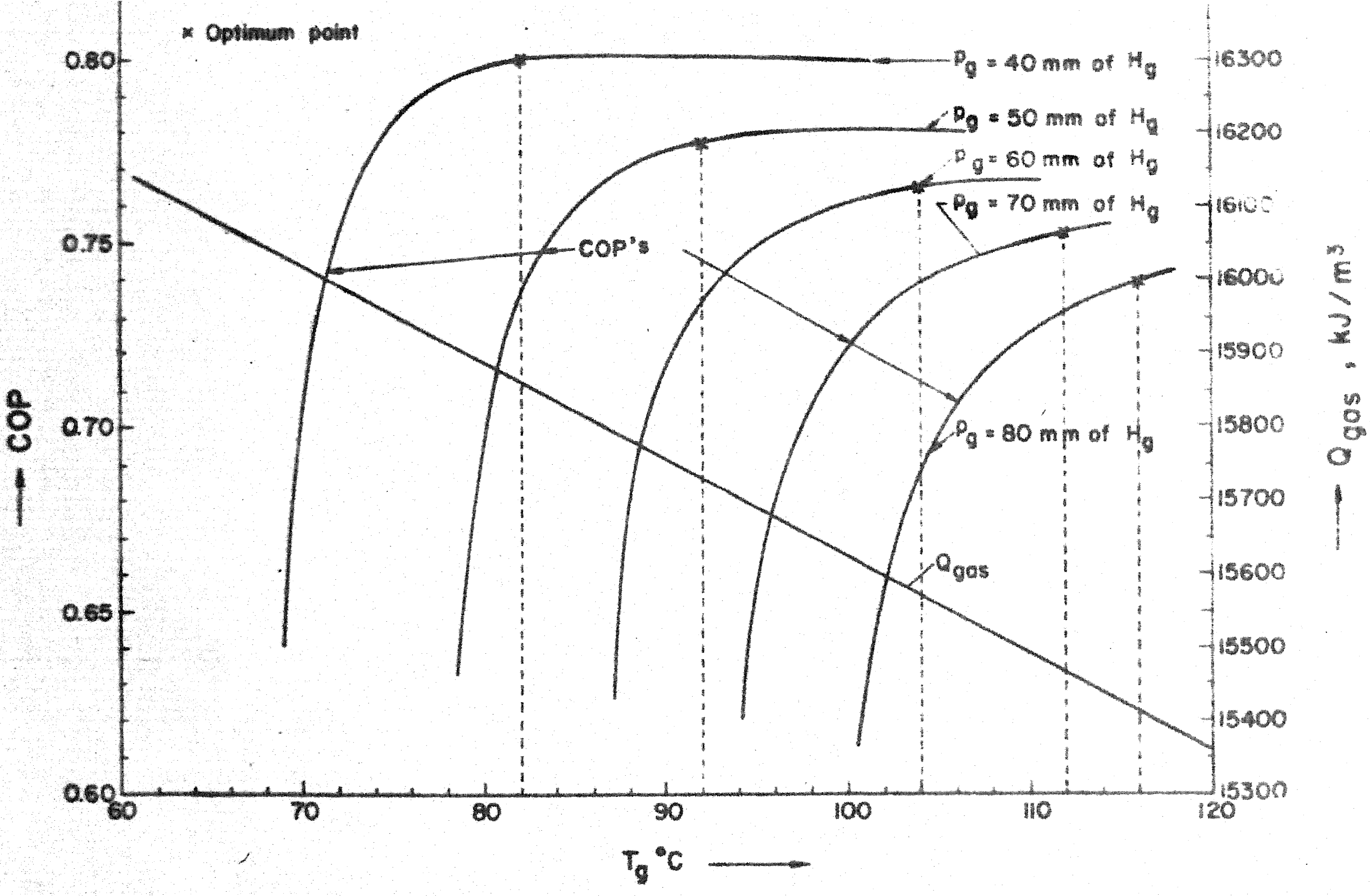

Fig.2.2 Variation in (COP's) with generator temperature T_g for different pressures along with Q_{gas}.

by summing the present worth of each of the payments of amount C_2.

Thus, $$P = \frac{C_2}{L} \sum_{i=1}^{L} (1/(1 + R)^{L-1}) \qquad (2.35)$$

Eq. (2.35) being geometric progression of constant ratio $1/(1 + R)$,

then,

$$P = \frac{C_2}{L} [((1 + R)^L - 1)/(R(1 + R)^{L-1})] \qquad (2.36)$$

The total cost of biogas per year is given by

$$C_T = \left\{C_1 + C_2 [((1 + R)^L - 1)/(R (1 + R)^{L-1})]\right\} /L \quad \ldots \quad (2.37)$$

The optimum value yielding C_T minimum was computed using iterative method. The computer results for the same are given in Appendix-B.

CHAPTER - III

LOAD CALCULATIONS

3.1 Cooling Load Calculations

Perishable commodities for usage in day to day life are sometimes preserved for convenience to avoid spoilage. To produce comfort condition during hot season days refrigeration is required. For these purposes LiBr-H_2O system has been selected. The capacity of the system is decided on the basis of cooling load calculations. The details are as follows:

(i) Cooling load due to commodities

  (a) continuous commodity load

  (b) intermittent commodity load.

(ii) Structure load.

Cooling load due to commodities:

The heat release from the commodity comprises sensible cooling of products from the ambient temperature to freezing temperature, enthalpy of freezing, sensible cooling below freezing and heat of respiration [19]. Since water is used as a refrigerant, the system would operate above freezing temperature. Hence, the heat

release from the commodities for storage above 0°C reduces to,

$$Q_{cod} = M\,[C_p\,(T_{am} - T_{store})]\,/\,(CF \times t) + M.hr/1000 \quad \ldots \quad (3.1)$$

where

Q_{cod}	=	heat release from the commodity in kJ/h
M	=	amount of the commodity stored in kg
C_p	=	specific heat of the commodity above freezing
T_{am}	=	ambient temperature (314.45 K)
T_{store}	=	storage temperature (278.15 K)
CF	=	chilling rate factor
t	=	chilling time
hr	=	energy release due to respiration per tonne mass per unit time.

The continuous commodity loads are due to the eatables which are stored for all 24 hours, such as, apple, tomato, crated eggs, fish, carrot, oranges, etc. The intermittent loads are due to commodities which are kept in the refrigerator at times, such as, milk, curd, water, etc. The parameters in Eq. (3.1) for different commodities are tabulated in table 3.1. The cooling load due to different commodities, Q_{cod}, is also tabulated. The values of parameters in table 3.1 are taken from [19,20,21].

Table 3.1

Design data for different commodities along with cooling load required for their storage

Parameters / Commodities	M (kg)	C_p (kJ/kg°C)	CF	t (h)	hr (kJ/ton-h)	Q_{cod} (kJ/h)
Apple	3	3.768	0.67	24	26.166	25.0
Tomato	1	3.85	1.0	24	54.26	5.88
Eggs(crated)	0.65	3.192	0.85	10	155.02	8.89
Fish	2	3.182	1.0	4	245.448	58.244
Carrot	2	3.6	0.8	24	122.103	13.857
Oranges	3	3.768	0.7	22	53.303	26.805
Milk	5	3.906	0.85	5	86.122	167.240
Curd	4	3.906	0.9	6	86.122	106.24
Water	5	h_{am}=171.75 h_{store}= 20.98	1.0	3	0	502.566

where, h_{am} and h_{store} are the enthalpies of water corresponding to temperatures T_{am} and T_{store}.

The total cooling load on summing the individual commodity loads comes out to be:

$$\bar{Q}_{cod} = 914.72 \simeq 915 \text{ kJ/h}$$

Structure load:

The size of the storage cabinet is assumed to be same as that of a 165 litre refrigerator.

Dimensions of the refrigerator:

Outer : 0.55 x 0.55 x 0.92 m

Inner : 0.45 x 0.45 x 0.82 m

Insulation: 0.05 m (glass wool).

Overall heat transfer coefficient for the cabinet is given by,

$$U_{o_b} = \frac{1}{\frac{1}{h_{i_b}} + \frac{1}{h_{o_b}} + \frac{\delta'_{wool}}{k_{wool}}} \qquad (3.2)$$

where h_{i_b} and h_{o_b} are respectively inner and outer heat transfer coefficients and are taken as: $h_{i_b} = h_{o_b} = 100$ kJ/hm^2°C and k_{wool} = thermal conductivity of the wool (= 0.15 kJ/hm^2°C).

δ'_{wool} = insulation thickness

Substituting respective values in Eq. (3.2) we have

$$U_{o_b} = 2.83 \text{ kJ/hm}^2\text{°C}$$

Also

$$Q_s = U_{o_b} A_{i_b} (T_{am} - T_{store}) \qquad (3.3)$$

where, Q_s is the structure load and A_{i_b} is the heat transfer area ($\simeq$ 4 x 0.45 x 0.82 + 2 x 0.45 x 0.45).

Substituting the respective values in Eq. (3.3), we have

$$Q_s = 193.233 \text{ kJ/h}$$

Increasing by 10% for safety, $Q_s = 213$ kJ/h

Hence, total cooling load $= \bar{Q}_{cod} + Q_s = 1128$ kJ/h

This load is the peak load, i.e. if all the commodities listed in table 3.1 are kept in the cabinet at a time. But the actual load will be fluctuating according to the requirement as shown in Fig.(3.1). From Fig. (3.1) $Q_{area} = 476$ kJ/h, but the maximum load as can be seen from the Fig.(3.1) is at 10 to 13 hours; on the basis of which the cabinet is to be designed,

i.e., $\dot{Q}_e = 593.333$ kJ/h $\simeq 600$ kJ/h

where $\dot{Q}_e$ is the rate of cooling load on the cabinet.

3.2 Energy Exchange for Components

Making use of the LiBr - concentration charts and equations the various parameters at pressure, $p_g = p_c = 80$ mm of H_g and evaporator temperature, $T_e = 5°C$ ($p_e = p_a = 6.6$ mm of H_g) are calculated and listed below:

Table 3.2

Property values at optimum generator temperature (T_{g_o}) corresponding to $p_g = 80$ mm of H_g, $T_e = 5°C$ and $\varepsilon_2 = 0.75$

T_{g_o} °C	$T_c = T_a$ °C	x_1	x_7	$h_1 = h_2$ kJ/kg	h_3 kJ/kg	h_4 kJ/kg	h_6 kJ/kg	h_7 kJ/kg	h_7' kJ/kg
116	47	61.4	69.0	136.8	2717.4	196.9	2510.1	300.1	182.5

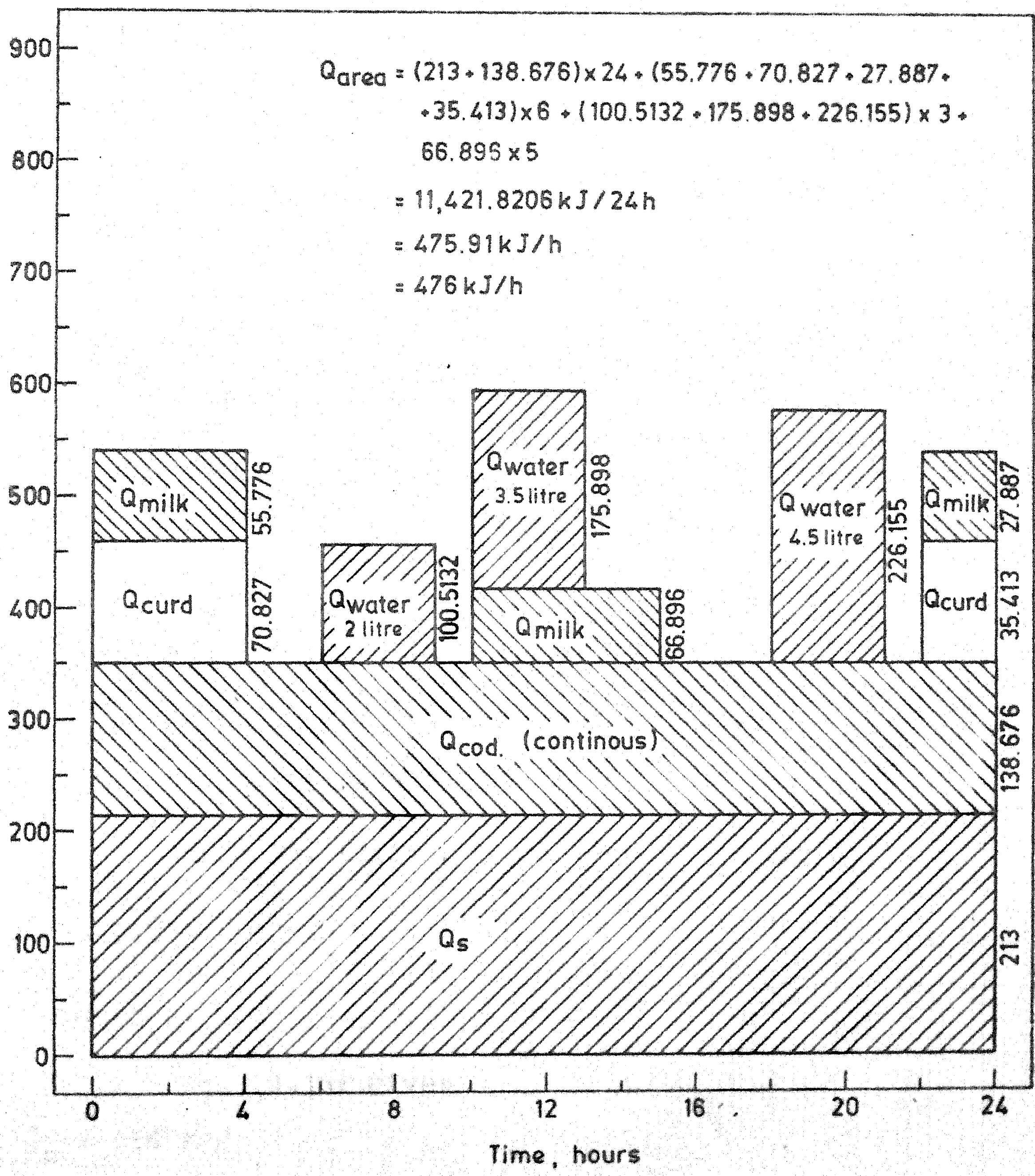

Fig. 3.1 Daily variation of cooling load.

The energy exchange due to different components, using Eqs. (2.1 to 2.15) and substituting the respective values from table 3.2, are as follows:

The capacity of the refrigerating unit, as calculated above is $\dot{Q}_e = 600$ kJ/h

Evaporator:

From Eq. (2.7) we have,

$Q_e = 2313.156$ kJ/kg and hence, $\dot{m}_6 = \dot{Q}_e/Q_e = 0.26$ kg/h

Absorber:

From Eqs. (2.4 to 2.6) we have,

$\dot{m}_1 = 2.361$ kg/h, $\dot{m}_7 = 2.101$ kg/h and $\dot{Q}_a = 715$ kJ/h

Generator:

From Eqs. (2.10 and 2.11) we have,

$\dot{m}_3 = \dot{m}_6$ and $\dot{Q}_g = 830$ kJ/h

From Eq. (2.14), COP $= \frac{Q_e}{Q_g} = \frac{\dot{Q}_e}{\dot{Q}_g} = 0.72$

$$TR = \frac{\dot{Q}_e}{12600} = 0.048$$

Condenser:

Eq. (2.15) gives,

$\dot{Q}_c = 656$ kJ/h

3.3 Biogas Requirement for the System

From Eq. (2.26), the useful gas required at the

optimum generator temperature, $T_{g_o} = 116°C$ is given as:

$$Q_{gas} = 15,400.41 \text{ kJ/m}^3$$

Hence, the volume of gas is given by Eqs. (2.33 and 2.34) as:

$$V = 0.048 \times 211680 \;/\; (0.72 \times 15,400.41) = 0.92 \text{ m}^3\text{/day}$$

CHAPTER - IV

SYSTEM DESIGN

The design of the vapour-absorption refrigeration system components require considerable informations such as feasibility of certain systems physical realizability, economic worthwhileness, financial feasibility, operating environmental conditions including chemical and physical reactions, etc. Besides these, one has to consider factors such as materials, components and their optimum combination and adaptability by customers. The cooling and component load calculations have already been discussed in Chapter-3.

4.1 Condenser Design

The condenser is the heat rejecting unit in a refrigerating system. When the saturated vapour comes in contact with a surface, at a temperature lower than the former, condensation occurs either in drops or as a film, [14]. The rate of heat flow depends on the condensate film thickness, which depends on the rate at which vapour is condensed and the rate of condensate removal. In the present case air cooled condenser has been selected due to simplicity. The condensate covers the inside tube

surface, flows by gravity, collects at the bottom of the inside horizontal tubes and flows by hydrostatic gradient. Chato [22] has obtained the following expression for condensation of refrigerants at low vapour velocities inside horizontal tubes as:

$$h_{i_c} = 0.555 \left[\frac{\rho_{l_c} (\rho_{l_c} - \rho_{v_c}) \, g \, k_{l_c}^3 \, h'_{lv_c}}{\mu_{l_c} \, d_{i_c} \, (T_{s_c} - T_{w_{i_c}})} \right]^{0.25} \quad \ldots. \quad (4.1)$$

in the range of

$$Re_c = \frac{d_{i_c} \, G_{v_c}}{\mu_c} < 35{,}000$$

where Re_c is evaluated at inlet conditions to the tube

and

$$h'_{lv_c} = h_{lv_c} + 0.68 \, C_{p_{w_c}} \, (T_{s_c} - T_{w_{i_c}}) \qquad (4.2)$$

where

h_{lv_c} = latent heat of condensation

h'_{lv} = effective latent heat of condensation allowing for the effect of superheat.

The tube and fin dimensions, selected, are tabulated in table 4.1.

Table 4.1

Tube and Fin dimension of the condenser

Tube dimensions					Fin dimensions		
d_{i_c} (m) $\times 10^{-2}$	d_{o_c} (m) $\times 10^{-2}$	r_{i_c} (m) $\times 10^{-2}$	r_{o_c} (m) $\times 10^{-2}$	δ'_c (m) $\times 10^{-2}$	$\bar{l}_c$ (m) $\times 10^{-2}$	r_c (m) $\times 10^{-2}$	δ_c (m) $\times 10^{-3}$
1.43	1.67	0.715	0.835	0.12	2.8675	4.175	0.42

The heat-transfer coefficient for the water-vapour flow on the inside of the tube is determined from the flow conditions with properties evaluated at bulk temperature. The free-convection heat-transfer coefficient on the outside of the tube depends on the temperature difference between the surface and the ambient air. The heat transfer area is increased by using fins.

The properties of saturated water at $T_{s_c} = 47°C$ [23,24] are given by table 4.2.

Table 4.2

Properties of saturated water at $T_{s_c} = 47°C$

k_{l_c} (kJ/m-h-°C)	μ_{l_c} (kg/m-h)	μ_{v_c} (kg/m-h)	ρ_{l_c} (kg/m^3)	ρ_{v_c} (kg/m^3)	h_{lv_c} (kJ/kg)	$C_{p_{w_c}}$ (kJ/kg°C)
2.322	2.232	0.0468 (at 116°C)	989.61	0.071	2391.2	4.1868

The Reynold number is

$$Re_a = \frac{d_{i_c} G_{v_c}}{\mu_{v_c}} = \frac{d_{i_c} (\dot{m}_3 / \frac{\pi}{4} d_{i_c}^2)}{\mu_{v_c}} = 1179.574$$

where, $\dot{m}_3$ = mass flow rate of water vapour in the condenser ($\simeq$ 0.26 kg/h)

and since Re < 35,000, using Eq. (4.1) and substituting values from tables (4.1 and 4.2) we have,

$$h_{i_c} = 8250.394 \left(h'_{lv_c} / (47 - T_{w_{i_c}})\right)^{0.25} \qquad (4.3)$$

and

$$h'_{lv_c} = 2391.2 + 0.68 \times 4.1868 \,(47 - T_{w_{i_c}}) \qquad (4.4)$$

Now, the temperatures, $T_{w_{i_c}}$, T_{w_o} and T_f are unknown, hence iterative procedure is followed to find the former and hence, heat transfer coefficients h_i, h_o and h_f are calculated.

Iteratively, $T_{w_{i_c}} = 46.97°C$

Hence, Eqs. (4.3 and 4.4) give:

$\therefore$ h'_{lv_c} = 2391.2854 kJ/kg and h_{i_c} = 138,628.406 kJ/m^2-h-°C

Heat transfer coefficient on fin side having free convection is expressed as [25]

$$Nu = c\,(Gr \,.\, Pr)^n \qquad (4.5)$$

The product Gr. Pr depend upon the fluid properties, the temperature difference between the surface and the fluid

and the characteristic length of the surface. The constant c and exponent n depend upon physical configuration and nature of flow.

Simplified equations for air as heat transport fluid, reported by [14, 23, 26, 27] are given below:
For small cylinders, laminar range ($10^4 < Gr\ Pr < 10^9$)

$$h_{o_c} = 4.752\ (\ \Delta T'_c\ /\ d_{o_c}\ )^{0.25} \tag{4.6}$$

and for vertical plates (for finned surfaces), laminar range (same range as above)

$$h_{f_c} = 5.112\ (\Delta T''_c\ /\ \bar{l}_c)^{0.25} \tag{4.7}$$

where, h_{o_c} and h_{f_c} are heat transfer coefficients outside the tube and the fin, respectively and $\Delta T' = T_{w_{o_c}} - T_{am}$;
$\Delta T''_c = T_{f_c} - T_{am}$

Design ambient temperature for Kanpur city is $T_{am} = 41.3°C$
By iterative procedure I got $T_{w_{o_c}} = 46.96°C$ and $T_{f_c} = 46.5°C$

$\therefore\ h_{o_c} = 20.3893\ kJ/m^2\text{-}h\text{-}°C$ and $h_{f_c} = 18.7593\ kJ/m^2\text{-}h\text{-}°C$

The overall heat transfer coefficient [28] is given by:

$$\frac{1}{U_{f_{o_c}}} = FF_c\ [\frac{1}{h_{i_c}} + \frac{\delta_c}{k_{w_c}}] + \frac{1}{h_{red_c}} \tag{4.8}$$

where,

$$FF_c = (A_{f_c} + A_{o_c})\ /\ A_{i_c}$$

and

$$A_{f_c} = 2\ \pi\ n_c\ [(r_c + \delta_c/2)^2 - r_{o_c}^2]$$

$$A_{o_c} = 2\ \pi\ L_c\ (1 - n_c\ \delta_c)\ r_{o_c} \qquad (4.9)$$

$$A_{i_c} = 2\ \pi\ r_{i_c}\ L_c$$

$$h_{red} = (h_{f_c}\ \phi_c\ A_{f_c} + h_{o_c}\ A_{o_c}) / (A_{f_c} + A_{o_c})$$

... (4.10)

and thermal conductivity,

k_{w_c} = 1381.3 kJ/h-m-°C for copper tube wall.

Assuming, number of fins n_c mounted per unit length of the tube to be 72, the areas A_{i_c} , A_{o_c} and A_{f_c} per unit length are calculated as:

A_{f_c} = 0.76495 m^2 , A_{o_c} = 0.050878 m^2, A_{i_c} = 0.04492477 m^2

and FF_c = 18.16.

To account for the variation in the heat flux due to temperature difference at the tip and the root of the fin, fin effectiveness, ϕ_c , is defined. For constant thickness square fins the efficiency of a constant thickness annular fin of the same area can be used [29]. More accuracy, particularly with rectangular fins of large aspect ratio, can be obtained by dividing the fin into circular section [30]. From the fin efficiency curves

from Fig. (2.11) in [28], ϕ_c are found for the particular values of r_c^* and Ψ_c

where,

$$r_c^* = \frac{r_c + \delta_c/2}{r_{o_c}} \tag{4.11}$$

$$\Psi_c = \bar{l}_c \sqrt{h_{f_c}/(k_{f_c} \cdot \delta_c/2)} \tag{4.12}$$

Taking, thermal conductivity,

k_{f_c} = 737.355 kJ/m-h-°C for Aluminium fin and substituting respective values in Eqs. (4.11 and 4.12), we have

r_c^* = 5.025 and Ψ_c = 0.316 and correspondingly ϕ_c = 0.93

Substituting the respective values in Eqs. (4.8 and 4.10)

h_{red_c} = 17.63 kJ/m^2-h-°C and $U_{f_{o_c}}$ = 17.5845 kJ/m^2-h-°C

Heat transfer rate per unit length of the condenser is given by:

$$q_c = U_{f_{o_c}} \times (A_{f_c} + A_{o_c}) \times (T_{s_c} - T_{am}) \tag{4.13}$$

Substituting the respective values in Eq. (4.13) we have,

$$q_c = 17.5845 \times (0.76495 + 0.050878) \times (47 - 41.3)$$
$$= 81.7718 \text{ kJ/h}$$

Since the heat rejected from the condenser is $\dot{Q}_c$ = 656 kJ/h

the length of the finned copper tube required for the complete condensation of the water vapour is:

$$L_c = \dot{Q}_c/q_c = 8.0 \text{ m}$$

Now, this length of tube has to be arranged such as to have a compact volume of the condenser. This can be arranged in two columns and six rows, so that the condenser length is equal to 0.52 m and the rest tube is used in eleven bends. The assumed 72 fins per m length are to be mounted on 0.78 m length. Hence, the spacing to be kept is 10.83×10^{-3} m.

4.2 Absorber Design

The main function of the absorber is to cool and totally condense the refrigerant vapour coming from the evaporator. The strong LiBr - water solution becomes a weak solution. This equipment is also called as absorber-condenser. In the simplest [31] absorber condenser design, the refrigerant vapours and the absorbent liquid are fed through an efficient mixer to the top of the heat exchanger and withdrawn from the bottom as a complete condensed liquid at, or slightly below, its saturation temperature. The most efficient heat transfer arrangement for this purpose is with the vapour liquid mixture flowing downward in a single pass inside vertical tubes surrounded by cooling water. This would be much costlier arrangement

due to high cost of maintenance for a small unit like the present one.

In the air cooled absorber-condenser the vapour liquid mixture flows inside a series of finned tubes, the air is blown across the tube bank and heat due to absorption of water vapour gets rejected. In its design, the conventional methods for calculating heat transfer and pressure drops for condensation inside tubes may be used. The specific correlations are decided according to vertical or horizontal orientation of the tube.

In the present work air cooled absorber has been selected due to low maintenance cost and to eliminate the use of electricity as in many rural areas electricity is not available. The strong LiBr - water solution and the refrigerant vapour enter the top of the absorber, rendering parallel - two phase flow inside the tube. The LiBr solution which flows inside finned tubes, gets cooled due to natural correction. As the vapour gets absorbed during the process it is similar to two phase condensation.

The design of the absorber follows the same procedure as in case of condenser design. Rewriting the equations for the absorber side.

Heat transfer coefficient inside horizontal tube,

$$h_{i_a} = 0.555 \left[\frac{\rho_{l_a} \cdot (\rho_{l_a} - \rho_{v_a}) g \, k_{l_a}^3 \cdot h'_{lv_a}}{\mu_{l_a} \, d_{i_a} \, (T_{s_a} - T_{w_{i_a}})} \right]^{0.25} \qquad (4.14)$$

The properties of LiBr-water solution [32] and water vapour at the designed conditions are given in table 4.3. The tube and fin dimensions selected are given in table 4.4.

Table 4.3

Properties of $LiBr-H_2O$ solution and water vapour

$LiBr-H_2O$ solution at 61.4% conc. and $T_{s_c} = 47°C$				Sat. water vapour at $T_{s_c} = 47°C$		
ρ_{l_a} (kg/m^3)	k_{l_a} (kJ/m-h-°C)	μ_{l_a} (kg/m-h)	C_{p_L} (kJ/kg°C)	ρ_{v_a} (kg/m^3)	h_{lv_a} (kJ/kg)	μ_{v_a} (at 5°C) (kg/m-h)
1730	1.686	18.72	1.84	0.0705	2391.2	0.0324

Table 4.4

Tube and fin dimensions for the absorber

Tube dimensions					Fin dimensions		
d_{i_a} (m) $\times 10^{-2}$	d_{o_a} (m) $\times 10^{-2}$	r_{i_a} (m) $\times 10^{-2}$	r_{o_a} (m) $\times 10^{-2}$	δ'_a (m) $\times 10^{-2}$	$\bar{l}_a$ (m) $\times 10^{-2}$	r_a (m) $\times 10^{-2}$	δ_a (m) $\times 10^{-3}$
1.508	1.968	0.754	0.984	0.23	3.374	4.895	0.58

The Reynolds number is given by:

$$Re_a = \frac{d_{i_a} \; G_{\bar{v}_a}}{\mu_{v_a}} = \frac{d_{i_a} \times (\dot{m}_6 \,/\, (\frac{\pi}{4}\, d_{i_a}^2))}{\mu_{v_a}} = 677.54 < 35{,}000$$

Similarly,

$$h'_{lv_a} = h_{lv_a} + 0.68\; C_{p_L}\; (T_{s_a} - T_{w_{i_a}}) \qquad (4.15)$$

Again the unknown temperatures T_{w_i}, T_{w_o}, T_f are evaluated using interative method, hence h_i, h_o and h_f are obtained. Substituting values from tables (4.3 and 4.4) in Eqs.(4.14 and 4.15), we have,

$$h_{i_a} = 4976.682 \left[\frac{h'_{lv_a}}{47 - T_{w_{i_a}}} \right]^{0.25} \qquad (4.16)$$

and

$$h'_{lv_a} = 2391.2 + 0.68 \times 1.84 \times (T_{s_a} - T_{w_{i_a}}) \qquad \ldots (4.17)$$

Iteratively,

$$T_{w_{i_a}} = 46.97°C$$

$$\therefore \quad h'_{lv_a} = 2391.2 \text{ kJ/kg}$$

and

$$h_{i_a} = 83621 \text{ kJ/m}^2\text{-h-°C}$$

Rewriting the Eqs. (4.6 and 4.7) for outer heat transfer coefficients across tubes and vertical plate fins respectively, we have

(a)
$$h_{o_a} = 4.752 \left(\frac{\Delta T'}{d_o}\right)_a^{0.25} \text{ kJ/m}^2\text{-h-°C} \qquad (4.18)$$

(b) $$h_{f_a} = 5.112 \left(\frac{\Delta T''}{\bar{I}}\right)_a^{0.25} \quad kJ/m^2\text{-}h\text{-}^\circ C \tag{4.19}$$

$$(\Delta T')_a = (T_{w_{o_a}} - T_{am}) \; ; \; T_{am} = 41.3^\circ C$$

$$(\Delta T'')_a = (T_{f_a} - T_{am})$$

From iteration

$$T_{w_{o_a}} = 46.95^\circ C \text{ and } T_{f_a} = 45.6\ ^\circ C$$

Therefore,

$$h_{o_a} = 19.56\ kJ/m^2\text{-}h\text{-}^\circ C \text{ and } h_{f_a} = 17.18\ kJ/m^2\text{-}h\text{-}^\circ C$$

Rewriting Eq. (4.8) for absorber side,

$$\frac{1}{U_{f_{o_a}}} = FF_a \left[\frac{1}{h_{i_a}} + \frac{\delta'_a}{k_{w_a}}\right] + \frac{1}{h_{red_a}} \tag{4.20}$$

$$FF_a = (A_{f_a} + A_{o_a}) / A_{i_a}$$

$$A_{f_a} = 2\ \pi\ n_a \left[(r_a + \delta_a/2)^2 - r_{o_a}^2\right] \tag{4.21}$$

$$A_{o_a} = 2\ \pi\ L_a\ (1 - n_a\,\delta_a)\ r_{o_a}$$

$$A_{i_a} = 2\ \pi\ r_{i_a}\ L_a$$

$$h_{red_a} = (h_{f_a}\ \emptyset_a\ A_{f_a} + h_{o_a}\ A_{o_a})/(A_{f_a} + A_{o_a}) \quad \ldots . \tag{4.22}$$

Assuming, n_a = 84/unit length and substituting the respective values in Eqs. (4.21 and 4.22), we have $A_{f_a} = 1.2285\ m^2$, $A_{o_a} = 0.0588\ m^2$, $A_{i_a} = 0.0474\ m^2$ and $FF_a = 27$.

The conductivity of mild steel (for tube), $k_{w_a} = 193.0$ (at 47°C) and the conductivity of G.I. Sheet (for fin), $k_{f_a} = 209.4$ (at 41.3°C) in kJ/m-h-°C.

Similarly, the parameters:

$$r_a^* = (r_a + \delta_a/2)/r_{o_a} \tag{4.23}$$

$$\Psi_a = \bar{l}_a \sqrt{h_{f_a}/(k_{f_a} \cdot \delta_a/2)} \tag{4.24}$$

Substituting respective values in Eqs. (4.21 and 4.22) we have, $r^* = 5.0$ and $\Psi_a = 0.512$ and correspondingly $\phi_a = 0.8$.

Eq. (4.22) gives , $h_{red} = 14.0$ kJ/m^2-h-°C

Substituting values in Eq. (4.20) we have,

$$U_{f_{o_a}} = 13.9 \text{ kJ/m}^2\text{-h-°C}$$

Since,

$$q_a = U_{f_{o_a}} A_{f_{o_a}} (T_{s_a} - T_{am}) \tag{4.25}$$

$$= 13.9 \times 1.2285\ (47 - 41.3) = 97.334 \text{ kJ/h}$$

Now heat of absorption is found as $\dot{Q}_a = 715$ kJ/h

Hence, length of finned mild steel tube required is:

$$L_a = \frac{\dot{Q}_a}{q_a} = 715/97.334 = 7.35 \text{ m}$$

Total number of fins = 7.35 x 84 = 618

It is assumed that the number of fins, $n_a = 84$/m length,

in order to minimise the space occupied by the absorber, it may be arranged in different rows.

Let 6 m length tube be finned and rest be used in bends etc.

Thus, 618 fins are to be mounted on 6 m tube,

i.e., On 1 m tube, fins mounted = 103 with spacing approximately 9.7 mm

4.3 Evaporator Design

As the refrigerant enters the evaporator through the throttle valve, it starts boiling as shown in Fig. 5.1 [33]. It is assumed in this analysis that the pressure drop along the tube is small compared to the static pressure rendering constant saturation temperature in the evaporator. Heat transfer coefficient to single phase liquid under forced convection is given as [33]:

$$h_{i_e} = 0.17\,[k_1/d_i]_e\,[G_1 . d_i/\mu_1]_e^{0.33}\,[c_{p_1} . \mu_1/k_1]_e^{0.43}\,[p_{r_1}\,/\,p_{r_w}]_e^{0.25}\,[d^3_i\,\rho^2_1\,g\,\beta\,\Delta T\,/\mu^2_1]_e^{0.1} \quad \ldots \quad (4.26)$$

This relationship is valid for heating in vertical upflow or cooling in vertical downflow for L/d > 50 and $[\frac{Gd}{\mu_1}] < 2000$. It also accounts for the influence of free convection. The properties of saturated liquid at $T_e = 5°C$ are given in table 4.5.

Table 4.5

ρ_{l_e} (kg/m^3)	k_{l_e} (kJ/m-h-°C)	μ_{l_e} (kg/m-h)	$C_{p_{l_e}}$ (kJ/kg°C)	d_{i_e} (m) x 10^{-2}	d_{o_e} (m) x 10^{-2}
999.9	2.08	6.48	4.19	1.268	1.608

where,

$$G_{l_e} = \dot{m}_6/(\frac{\pi}{4}\, d_{i_e}^2)$$

$$\beta = 1/(273.15 + 5) \text{ and } \Delta T = (T_{w_{i_e}} - T_{s_e})$$

Substituting the respective values G_{l_e} = 2058.95 kg/m^2-h and β = 3.6 x 10^{-3}.

For small diameter tubes, fluid properties at the wall surface are approximately same as at the bulk stream, so that p_{r_l}/p_{r_w} = 1.0.

T_{w_i} and T_{w_o} are the unknown temperatures which are calculated iteratively, hence, h_i and h_o.

Substituting the respective values in Eq. (4.26) we have,

$$h_{i_e} = 362.84\ (\Delta T)^{0.1} \tag{4.27}$$

By iteration, $T_{w_{i_e}}$ = 7.519°C and h_{i_e} = 397.96 kJ/m^2-h-°C

Heat transfer coefficient for helical coil [34],

$$h_{i_{e_x}} = h_{i_e} \times 1.127 = 448.5 \text{ kJ/m}^2\text{-h-°C}$$

Outside tube heat transfer coefficient by natural convection is given by [14] as:

$$Nu = 0.53\,[Gr\ .\ Pr]^{0.25} \qquad (4.28)$$

for $Gr.Pr = 10^4$ to 10^9

or

$$h_{o_e} = [\frac{k_{o_e}}{d_{o_e}}] \times 0.53 \times [\frac{g\ \beta\ \ \Delta T'_e\ \ d^3_{o_e}}{\nu^2_e} \times Pr]^{0.25} \qquad \ldots \qquad (4.29)$$

where, $\Delta T'_e = (T_{\infty_e} - T_{w_{o_e}})$

Properties of water at 8°C taken from [24] are tabulated in table 4.6.

Table 4.6

Properties of water at $T_{\infty_e} = 8°C$

k_{o_e} (kJ/m-h-°C)	ν_e (m^2/h) x 10^{-3}	Pr	β
2.05	5.3	10.97	$\frac{1}{(273.15+8)}$

Substituting values in Eq. (4.29) we have,

$$h_{o_e} = 1979.69\ (\ \Delta T'_e)^{0.25} \qquad (4.30)$$

For helical coil

$$h_{o_{e_x}} = 2231.1106\ (\ \Delta T'_e)^{0.25} \qquad (4.31)$$

By iteration, $T_{w_{o_e}} = 7.52°C$, and $h_{o_{e_x}} = 1857.08$ kJ/m^2-h-°C

Overall heat transfer coefficient is given by

$$\frac{1}{U_{o_e}} = \frac{A_{o_e}}{A_{i_e}} \times \left[\frac{1}{h_{i_e}} + \frac{\delta'_e}{k_{w_e}} \right] + \frac{1}{h_{o_e}} \qquad (4.32)$$

The inner and outer areas per unit length using table 4.5, are:

$$A_{i_e} = \pi\, d_{i_e}\, L_e = 0.0398\ m^2$$

$$A_{o_e} = \pi\, d_{o_e}\, L_e = 0.051\ m^2$$

Since $\delta'_e = 1.7 \times 10^{-3}$ m and the thermal conductivity of copper, $k_{w_e} = 1392.6$ kJ/m-h-°C

Substituting the respective values in Eq. (4.32) we have,

$$U_{o_e} = 296.956\ kJ/m^2\text{-}h\text{-}°C$$

Total refrigeration load on the evaporator,

$$\dot{Q}_e = 600\ kJ/h$$

or

$$\dot{Q}_e = U_{o_e} \times \pi \times d_{o_e} \times L_e \times (\Delta T_e) \qquad (4.33)$$

where $\Delta T_e = (T_{\infty_e} - T_{s_e})$

Substituting respective values, length of the evaporator tube, $L_e = 13$ m.

For the design of a refrigerator for a certain value of $\dot{Q}_e$, finned coil can be used. In the design of it h_{i_e} be calculated from Eq. (4.26) and h_o and h_f from Eqs. (4.6 and 4.7), and the same procedure may be adopted

as in the design of the condenser and the absorber. If the water is to be cooled at 10°C, then the properties of water at 10°C would yield,

$$h_{o_{e_x}} = 8041.044 \text{ kJ/m}^2\text{-h-°C}$$

The value of $h_{i_{e_x}}$ and other dimensions remaining same,

$$U_{o_e} = 338.483 \text{ kJ/m}^2\text{-h°C}$$

and the length of the evaporator tube,

$$L_e = 11.0 \text{ m}$$

4.4 Generator Design

The heat transfer to generator renders the release of superheated water vapour. The generator is designed for operating pressure of 80 mm of H_g and T_{g_o} of 116°C. For this $x_1 = 61.4\%$, $x_3 = 0$, $x_7 = 69\%$.

For $m_1 = 1$ kg/h

$m_3 = 0.11$ kg/h

The change in quality of vapour in the generator is found to be

$$\bar{x} = \frac{0 + m_3}{2} = 0.055$$

From the flow pattern as shown in Figures (1.2 and 1.4) in [33] it is seen that the flow is bubbly flow for this quality of vapour.

The relation for boiling with bubbles [14] can be written as

$$Nu = \frac{1}{C_{s_f}} (Re)^{0.667} (Pr)^{-0.7} \tag{4.34}$$

where,

$$Nu = (h_i\ D_b/k_l)_g\ ,\ Pr = (\mu_l\ C_{p_l}/k_l)_g\ ,$$

$$Re = \left(\frac{\dot{Q}_g}{A\ h_{lv}} \cdot \frac{D_b}{\mu_l} \right)_g \quad \text{and} \quad D_b = \sqrt{\frac{\sigma_t}{(\rho_l - \rho_v)}}_g \quad \ldots \tag{4.35}$$

Whenever possible it is recommended [33,35] that a pool boiling experiment be carried out to determine the value of C_{s_f} applicable to the particular conditions of interest. In the absence of such information a value of $C_{s_f} = 0.013$ may be used as a first approximation. The value of C_{s_f} for the water-polished stainless steel [27] is 0.0132.

The values of the various parameters taken from [14,24,32] at 61.4% concentration and generator temperature, $T_g = 116°C$ are given in table 4.7

Table 4.7

Property values of LiBr-H_2O and water vapour (at 116°C and 64.1%)

σ_t (N/m) x 10^{-3}	k_{l_g} (kJ/m-h-°C)	μ_{l_g} (kg/m-h)	$c_{p_{l_g}}$ (kJ/kg°C)	ρ_{l_g} (kg/m^3)	ρ_{v_g} (kg/m^3)
68.4	1.78	7.2	1.84	1.68x10^3	0.056

where,

σ_t = surface tension of water

ρ_{v_g} = density of water vapour

and

$C_{p_{l_g}}$, μ_{l_g} , k_{l_g} , ρ_{l_g} are respectively

specific heat, dynamic viscosity, thermal conductivity and density of LiBr-H_2O solution.

Substituting the respective values, in Eq. (4.34) we have,

$$D_b = \sqrt{\frac{68.434 \times 10^{-3}}{(1.68 \times 10^3 - 0.056\,) \times 9.81}} = 2.038 \times 10^{-3} \text{ m}$$

For $\dot{Q}_g$ = 830 kJ/h and tube dimensions as in table 4.8 we have,

$$A_{o_g} = \frac{\pi}{4} (2.068 \times 10^{-2})^2 = 3.3588 \times 10^{-4} \text{ m}^2$$

and

$$h'_{lv} = 2391.2 + 0.68 \times C_{p_{l_g}} \times (T_{w_{o_g}} - T_{s_g})$$

$$= 2391.2 + 0.68 \times 1.839 \times (120-116)$$

$$= 2396.2 \text{ kJ/kg.}$$

Table 4.8

Dimensions of generator tube

d_{i_g} (m) x 10^{-2}	d_{o_g} (m) x 10^{-2}	δ'_g (m) x 10^{-3}
1.68	2.07	1.96

Substituting values in Eq. (4.35) we have,

$Re = 0.292$ and

$Pr = 7.43$

Therefore, from Eq. (4.34) taking $C_{s_f} = 0.0132$ and putting respective values:

$$h_{i_g} = 7162.15 \text{ kJ/m}^2\text{-h-°C}$$

To heat the weak solution flowing through the generator heat is supplied by burning biogas inside the generator outer casing. The appropriate size of the generator has been calculated by iteration.

The first approximation assumes the length of the enclosure carrying a single tube (as an annulus) having $L_g = l_g = 0.305$ m. Let the inner diameter of the enclosure, $D_{i_g} = 0.13$ m and outer diameter of the tube, $d_{o_g} = 0.02068$ m. The shape factor was calculated as per [36]. It is found that $F_{1-2} = 1.4$ for the above dimensions. Here the enclosure is considered as body 2 and the tube as body 1. Heat transfer coefficient due to radiation is given by:

$$h_{r_g} = \frac{F_{1-2} \times \varepsilon_r \times \sigma \times [(T_{g_{av}} + 273.15)^4 - (T_{g_o} + 273.15)^4]}{(T_{g_{av}} - T_{g_o})} \quad \ldots \quad (4.36)$$

where, ε_r = emmissivity (approx. 1.0 for a black surface)

σ = Stephan Boltzman constant ($= 20.42 \times 10^{-8}$ kJ/m^2-h-K^4)

l_g = length of the enclosure, m

$T_{g_{av}}$ = average temperature of the flue gas in the enclosure

T_{g_o} = outer surface temperature of the tube.

If the flue gas is entering the enclosure at 166°C and leaving it at 145°C then, $T_{g_{av}} = 156°C$.

Substituting the respective values in Eq. (4.36) we have,

$$h_{r_g} = 79.4 \text{ kJ/m}^2\text{-h-°C}$$

Heat transfer coefficient due to free convection of air given as

$$h_{c_g} = 4.752\ (\Delta T_{m_g}/d_{o_g})^{0.25} \qquad (4.37)$$

Now LMTD,

$$\Delta T_{m_g} = \frac{166 - 145}{\ln\left(\frac{166-117}{145-117}\right)} = 37.53°C$$

Substituting values in Eq. 4.37 we have,

$$h_{c_g} = 31.02 \text{ kJ/m}^2\text{-h-°C}$$

Total outer heat transfer coefficient,

$$h_{o_g} = h_{r_g} + h_{c_g} = 110.407 \text{ kJ/m}^2\text{-h-°C}$$

$$\frac{1}{U_{o_g}} = \frac{d_{o_g}}{d_{i_g}}\left[\frac{1}{h_{i_g}} + \frac{\delta'_g}{k_g}\right] + \frac{1}{h_{o_g}} \quad \ldots \qquad (4.38)$$

Substituting the values in Eq. (4.38) we have,

$$U_{o_g} = 108.21 \text{ kJ/m}^2\text{-h-°C}$$

Using, $\dot{Q}_g = A_{o_g} \; U_{o_g} \; \Delta T_{m_g}$, we get

$$A_{o_g} = 0.204 \text{ m}^2$$

or

$$L_g = 3.14 \text{ m}$$

The length of the generator tube, L_g comes out to be 3.14 m which is more than the assumed value. For the next approximation four tubes were taken having the same dimensions kept within the same enclosure.

The shape factor, F_{1-2} , for this geometry is found graphically as shown in Fig.(4.1)and can be written as follows:

$$F_{1-2} = \frac{1}{A_1} \int_{A_1} \int_{A_2} \frac{\cos\theta_1 \cos\theta_2}{\pi S^2} \, d A_1 \, d A_2 \qquad (4.39)$$

Since, $\theta_1 = 0$ and the elemental area dA_1 of A_1 are equal segments, therefore,

$$F_{1-2} = \frac{1}{A_1} [dA_1 \sum_{j=1}^{8} \frac{\cos\theta_{2_j}}{\pi S^2_j} dA_{2_j} \quad] + \frac{1}{A_1'}[dA_1' \sum_{j=9}^{10} \frac{\cos\theta_{2_j}}{\pi S_j^2} dA_{2_j} \quad]$$

Substituting the values of θ and S we have, from Fig(4.1)

$$F_{1-2} = \frac{1}{A_1} [\; 2 \times \frac{dA_1}{\pi} \left\{ \frac{\cos(29)}{(0.056)^2} \times 0.044 + \frac{\cos(28)}{(0.039)^2} \times 0.03 \right.$$

$$\left. + \frac{\cos(20)}{(0.027)^2} \times 0.022 + \frac{\cos(8)}{(0.023)^2} \times 0.02 \right\} \times 0.305]$$

$$+ \frac{1}{A_1'} [2 \times \frac{dA_1'}{\pi} \left\{ \frac{\cos(11)}{(0.084)^2} \right\} \times 0.305]$$

From the Fig. (4.1), $dA_1/A_1 = 1/8$ and $dA_1'/A_1' = 1$

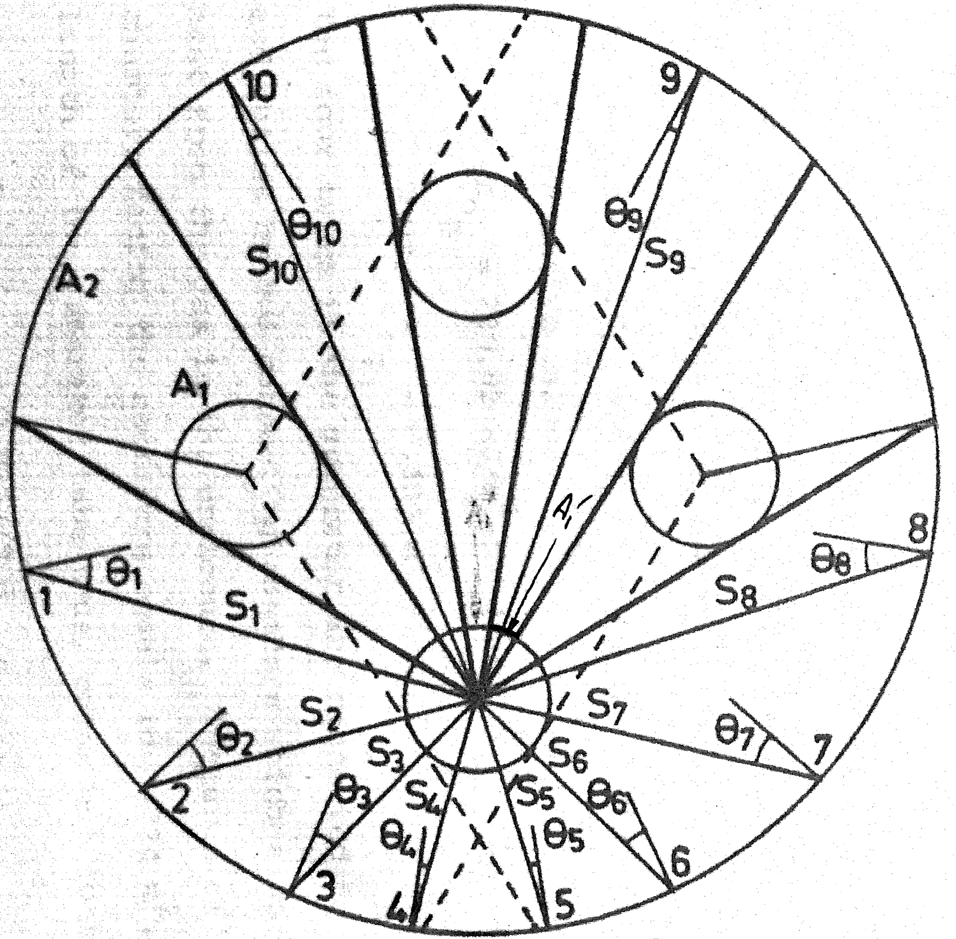

$\theta_1 = \theta_8 = 29^\circ$

$\theta_2 = \theta_7 = 28^\circ$

$\theta_3 = \theta_6 = 20^\circ$

$\theta_4 = \theta_5 = 8^\circ$

$\theta_9 = \theta_{10} = 11^\circ$

$S_1 = S_8 = 0.056\,m$

$S_2 = S_7 = 0.039$

$S_3 = S_6 = 0.027$

$S_4 = S_5 = 0.023$

$S_9 = S_{10} = 0.084$

Ratio 1:1

Fig. 4.1 Radiative heat exchange in the generator

Hence, $F_{1-2} = 3.4$.

It is seen from the Fig. (4.1) that the areas A_2 and A_2' of the enclosure seen by a single tube is also seen by the adjuscent two tubes, due to which net effect on a single tube is about 25% of the calculated value of the shape factor,

i.e., $F_{1-2} = 0.25 \times 3.4 = 0.85$

Hence, the heat transfer coefficient within the enclosure carrying four tubes is given by:

$$h_{r_g} = 4F_{1-2} \times \varepsilon_r \times \sigma \times \left[\frac{(T_{g_{av}} + 273.15)^4 - (T_{g_o} + 273.15)^4}{(T_{g_{av}} - T_{g_o})}\right]$$

Substituting the respective values we have,

$$h_{r_g} = 192.8 \text{ kJ/m}^2\text{-h-}^\circ\text{C}$$

The values of ΔT_{m_g} and h_{c_g} are same. On substitution of the respective values

$$h_{o_g} = 223.82 \text{ kJ/m}^2\text{-h-}^\circ\text{C and } U_{o_g} = 214.982 \text{ kJ/m}^2\text{-h-}^\circ\text{C.}$$

Thus, $A_{o_g} = 0.103 \text{ m}^2$

The four tubes in the generator are connected to the inlet and outlet by two connecting chambers which also receive heat from the gas in the enclosure. The area of the two chambers facing the enclosure equals to 0.024 m^2. The length of the generator tube thus, comes out to be:

$$L_g = (A_{o_g} - 0.024)/\pi\, d_{o_g} = 1.22 \text{ m}$$

This value is same as the assumed value.

4.5 Design of Preheater

The hot strong LiBr-H_2O solution returning from the generator is utilized for heating the weak solution coming from the absorber. This reduces the heat requirement in the generator. This also reduces the size of absorber heating area and enhances the absorption process. A counter flow heat exchanger is used. Brown and Gauvin [37] have developed a correlation for the mixed convection, laminar flow region.

$$Nu = 1.75 \; (\mu_b/\mu_w)^{0.14} \left[Gz + 0.012 \; (Gz \; Gr^{1/3})^{4/3}\right]^{1/3} \quad \ldots \quad (4.40)$$

where,

$Gz = Re \; Pr \; \frac{d}{L}$; μ_b and μ_w dynamic viscosities at the bulk temperature of solution and the tube wall.

Total heat transfer is determined from the energy absorbed by the cold fluid

$$\dot{Q}_p = \dot{m}_1 \cdot C_{p_{L_a}} \cdot \Delta T_m \quad (4.41)$$

Heat exchanger effectiveness,

$$\varepsilon_2 = \frac{\text{actual heat transfer}}{\text{maximum possible heat transfer}}$$

For counter flow, actual heat transfer,

$$\dot{Q}_p = \dot{m}_7 \cdot C_{p_{L_g}} \cdot (T_g - T_7') = \dot{m}_1 \cdot C_{p_{L_a}} \; (T_2' - T_a) \quad (4.42)$$

Maximum possible heat transfer,

$$\dot{Q}_{p_{max}} = (\dot{m}\, c)_{min.} (T_g - T_a) \qquad (4.43)$$

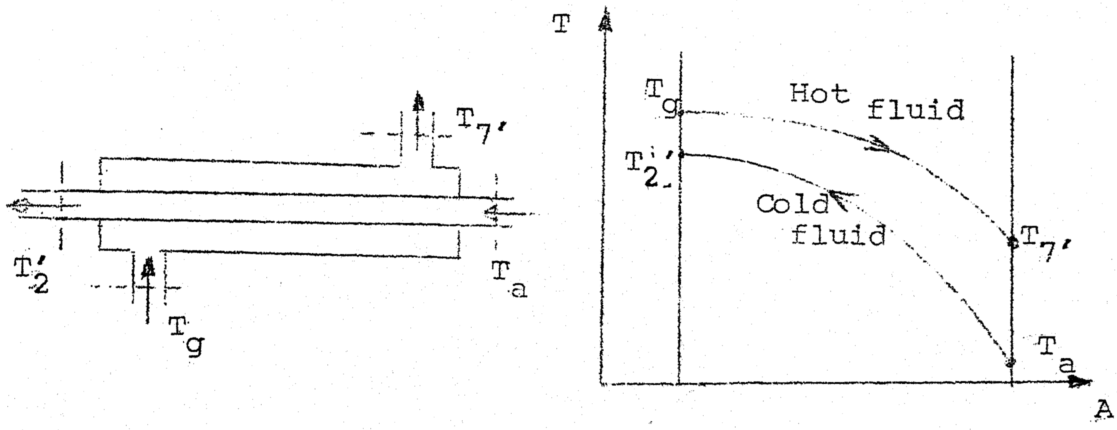

Fig. 4.2 : Temperature distribution in the preheater.

The specific heats of LiBr-H_2O solution at different concentrations are listed in table 4.9.

Table 4.9

Specific heats of LiBr-H_2O solution along with mass flow rates

$C_{p_{L_a}}$ kJ/kg°C	$\dot{m}_1$ kg/h	$C_{p_{L_a}} \cdot \dot{m}_1$ kJ/h-°C	$C_{p_{L_g}}$ kJ/kg°C	$\dot{m}_7$ kg/h	$C_{p_{L_g}} \cdot \dot{m}_7$ kJ/h-°C
1.839 (61.4%)	2.301	4.34	1.73 (69%)	2.361	3.64

From table 4.9, $\dot{m}_7\, C_{p_{L_g}}$ is minimum.

The unknown temperatures T_2' and T_7' are determined using effectiveness value, $\epsilon_2 = 0.75$

i.e. $$\varepsilon_2 = \{\dot{m}_1 \, C_{p_{L_a}} \, (T_2' - T_a)\} / \{\dot{m}_7 \cdot C_{p_{L_g}} \cdot (T_g - T_a)\} \quad \ldots \quad (4.44)$$

Also,

$$\varepsilon_2 = \{\dot{m}_7 \, C_{p_{L_g}} \, (T_g - T_7')\} / \{\dot{m}_7 \, C_{p_{L_g}} \, (T_g - T_a)\} \quad \ldots \quad (4.45)$$

Since $T_g = 116°C$ and $T_a = 47°C$,

substituting the respective values in Eqs. (4.44 and 4.45) we have,

$$T_2' = 90.34°C$$

and

$$T_7' = 64.25°C$$

The log mean temperature difference on substitution of respective values is given as:

$$\Delta T_m = \frac{(T_g - T_2') - (T_7' - T_a)}{\ln \dfrac{T_g - T_2'}{T_7' - T_a}} = 21.2°C$$

Th solution properties are taken at average temperatures fo evaluation of the heat transfer coefficient. Annulus (ho , strong solution), $T_h = (T_g + T_7')/2 = (116 + 64.25)/2 = 90.12°C$. Inner tube (cold, weak solution),

$$T_c = \frac{T_a + T_2'}{2} = \frac{47 + 90.34}{2} = 68.67°C$$

Properties of $LiBr-H_2O$ solution at different conditions are given in table 4.10.

Table 4.10

Properties of $LiBr-H_2O$ solution at different conditions

Annullar side (69% and 90.12°C)			Tube side (64.1% and 68.67°C)		
k_{o_p} kJ/m-h-°C	μ_{o_p}	ρ_{o_p} (kg/m^3)	k_{i_p} kJ/m-h-°C	μ_{i_p}	ρ_{i_p} (kg/m^3)
1.75	15.12	1858	1.748	12.24	1715

Assuming the following dimensions:

Annulus: $D_{i_p} = 2.841 \times 10^{-2}$ m ; $d_{o_p} = 2.068 \times 10^{-2}$ m

Area, $A_{a_p} = \frac{\pi}{4}(D_{i_p}^2 - d_{o_p}^2) = 2.98 \times 10^{-4}\ m^2$

Equivalent diameter,

$$D_{e_p} = \frac{D_{i_p}^2 - d_{o_p}^2}{D_{i_p}} = 1.336 \times 10^{-2}\ m$$

Tube, $d_{i_p} = 1.676 \times 10^{-2}$ m , $d_{o_p} = 2.068 \times 10^{-2}$ m

$$A_{i_p} = \frac{\pi}{4}\ d_{i_p}^2 = 2.206 \times 10^{-4}\ m^2$$

Carrying out the calculations for the annulus and the tube separately we have,

Annulus:

$$Re = \frac{G_{o_p}\ D_{e_p}}{\mu_{o_p}} = \frac{\dot{m}_7}{A_{a_p}} \times \frac{D_{e_p}}{\mu_{o_p}} = \frac{2.101 \times 1.336 \times 10^{-2}}{2.98 \times 10^{-4} \times 15.12} = 6.23$$

$$Pr_{o_p} = \frac{\mu_{o_p} \cdot C_{p_{L_g}}}{k_{o_p}} = \frac{15.12 \times 1.73}{1.75} = 14.944$$

$$G_{r_{o_p}} = \frac{g\ \beta_{o_p}\ \Delta T_m \cdot D^3_{e_p}\ \rho^2_{o_p}}{\mu^2_{o_p}} = 9.81 \times (3600)^2 \times \frac{1}{(90.12+273.15)}$$

$$\times \frac{21.2 \times (1.336 \times 10^{-2})^3 \times (1858)^2}{(15.12)^2} = 2.672 \times 10^5$$

Assuming length of preheater as 1 m

$$Gz_{o_p} = Re_{o_p} \cdot Pr_{o_p} \cdot \frac{D_{e_p}}{L_p} = \frac{6.23 \times 14.944 \times 1.336 \times 10^{-2}}{1.0} = 1.244$$

Let $\mu_b = \mu_w$

Substituting these values in Eq. (4.40) we have heat transfer coefficient on the annulus side:

$$h_{o_p} = 402.144 \text{ kJ/m}^2\text{-h-°C}$$

Tube:

$$Re_{i_p} = \frac{G_{i_p}\ d_{i_p}}{\mu_{i_p}} = \frac{\dot{m}_1}{A_{i_p}} \times \frac{d_{i_p}}{\mu_{i_p}} = \frac{2.361}{2.206 \times 10^{-4}} \times \frac{1.676 \times 10^{-2}}{12.24}$$

$$= 14.655$$

$$Pr_{i_p} = \frac{\mu_{i_p}\ C_{p_{L_a}}}{k_{i_p}} = \frac{12.24 \times 1.839}{1.748} = 12.876$$

$$Gr_{i_p} = \frac{g\ \beta_{i_p}\ \Delta T_m \times d^3_{i_p}\ \rho^2_{i_p}}{\mu^2_{i_p}} = 9.81 \times (3600)^2 \times \frac{1}{(68.67+273.15)}$$

$$\times \frac{21.2 \times (1.676 \times 10^{-2})^3 \times (1715)^2}{(12.24)^2} = 7.29 \times 10^5$$

$$Gz_{i_p} = Re_{i_p} \cdot Pr_{i_p} \cdot \frac{d_{i_p}}{L_p} = 14.655 \times 12.876 \times \frac{1.676\times10^{-2}}{1.0}$$

$$= 3.1626 \quad (L = 1.0 \text{ m})$$

Substituting the respective values in Eq. (4.40), heat transfer coefficient on the inner side:

$$h_{i_p} = 307.54 \text{ kJ/m}^2\text{-h-}^\circ\text{C}$$

The overall heat transfer coefficient in the preheater is:

$$\frac{1}{U_{o_p}} = \frac{D_{i_p}}{d_{i_p}} \cdot \frac{1}{h_{i_p}} + \frac{D_{i_p}}{2\ k_{w_p}} \times \ln\left(\frac{d_{o_p}}{d_{i_p}}\right) + \frac{D_{i_p}}{2\ k_{w_p}} \cdot \ln\left(\frac{D_{i_p}}{d_{o_p}}\right) + \frac{1}{h_{o_p}} \quad \text{.... (4.46)}$$

The conductivity of mild steel,

$$k_{w_p} = 193 \text{ kJ/m-h-}^\circ\text{C}$$

Substituting the respective values in Eq. (4.46) we have,

$$U_{o_p} = 124.47 \text{ kJ/m}^2\text{-h-}^\circ\text{C}$$

From Eq. (4.41)

$$\dot{Q}_p = 2.361 \times 1.839 \times 21.2 = 92.05$$

Using,

$$Q_p = U_{o_p} \cdot A_{o_p} \cdot \Delta T_m \quad (4.47)$$

and putting the respective values,

$$A_{o_p} = 0.035 \text{ m}^2 \quad \text{and} \quad L_p = 0.84 \text{ m}$$

Thus, the value of L_p taken equal to 1.0 m is correct.

4.6 Fabrication and Assembly

Table 4.11 shows the specifications of the different components of the system. Fig. (4.3) shows the schematic view of the set-up. The condenser, absorber, generator and preheater were fabricated by 'Kalyan Kooling Corporation', Kanpur. As the water vapour condenses in the condenser, it was fabricated from copper having Aluminium fins. The absorber was fabricated from mild steel tube having G.I. sheet fins as shown in Fig.(4.4). The generator was fabricated from mild steel tube of 16.8 mm inner diameter. Four tubes were welded in 130 mm inner diameter pipe. The exit of the generator has two outlets : one for vapour supply to the condenser and the other for return of strong solution to the absorber via preheater. The evaporator is a helical coil copper tube fabricated from 16.08 mm outer diameter and is immersed in a water tank. Generator, heat exchanger, and the water tank were thermally insulated.

The assembly of the whole system is shown in Fig. (4.4). To measure the operating pressures in the generator and evaporator sides, inclined tube mercury manometers have been used. The connection between generator and condenser is done using glass tubes for visual aid. A drain valve is provided at the lowest level in the preheater. The charging line is provided on the

absorber side. The absorber is placed on adjustable jacks and the connections to the frame are made through polythene tubes. This is done for adjustment of pressure difference between the absorber and the generator. Thermocouples are provided to measure temperature in the evaporator and the generator.

Table 4.11

Specifications of the system components

Components / Specifications	Condenser	Absorber	Evaporator	Generator	Preheater
Heat transfer rate, $\dot{Q}$ (kJ/h)	656	715	600	830	-
Tube dimensions:					**Tube:**
Length (m)	8.0	7.35	13.00	1.22	1.0
$d_o \times 10^{-2}$ (m)	1.67	1.968	1.608	2.073	2.068
$d_i \times 10^{-2}$ (m)	1.43	1.508	1.268	1.68	1.676
Material	copper	M.S.	Copper	M.S.	M.S
Square Fin dimensions:					**Annulus:**
$\bar{l} \times 10^{-2}$ (m)	2.8675	3.374			$D_i = 2.841 \times 10^{-2}$ m
$\delta \times 10^{-3}$ (m)	0.42	0.58			$D_o = 3.541 \times 10^{-2}$ m
Spacing (m) $\times 10^{-3}$	10.83	9.70			Material: M.S.
Material	Al.	G.I. sheet			

The biogas plant has been fabricated from a cylindrical drum having a floating top as shown in Fig. (4.5). The inlet for charging and exit for discharge of disgested gobar are provided. The gas from the plant is supplied to generator burner through a G.I. Sheet. Wet-test metre is provided to get the flow rate of biogas. The manometer is provided in the supply line of the biogas to get the supply pressure.

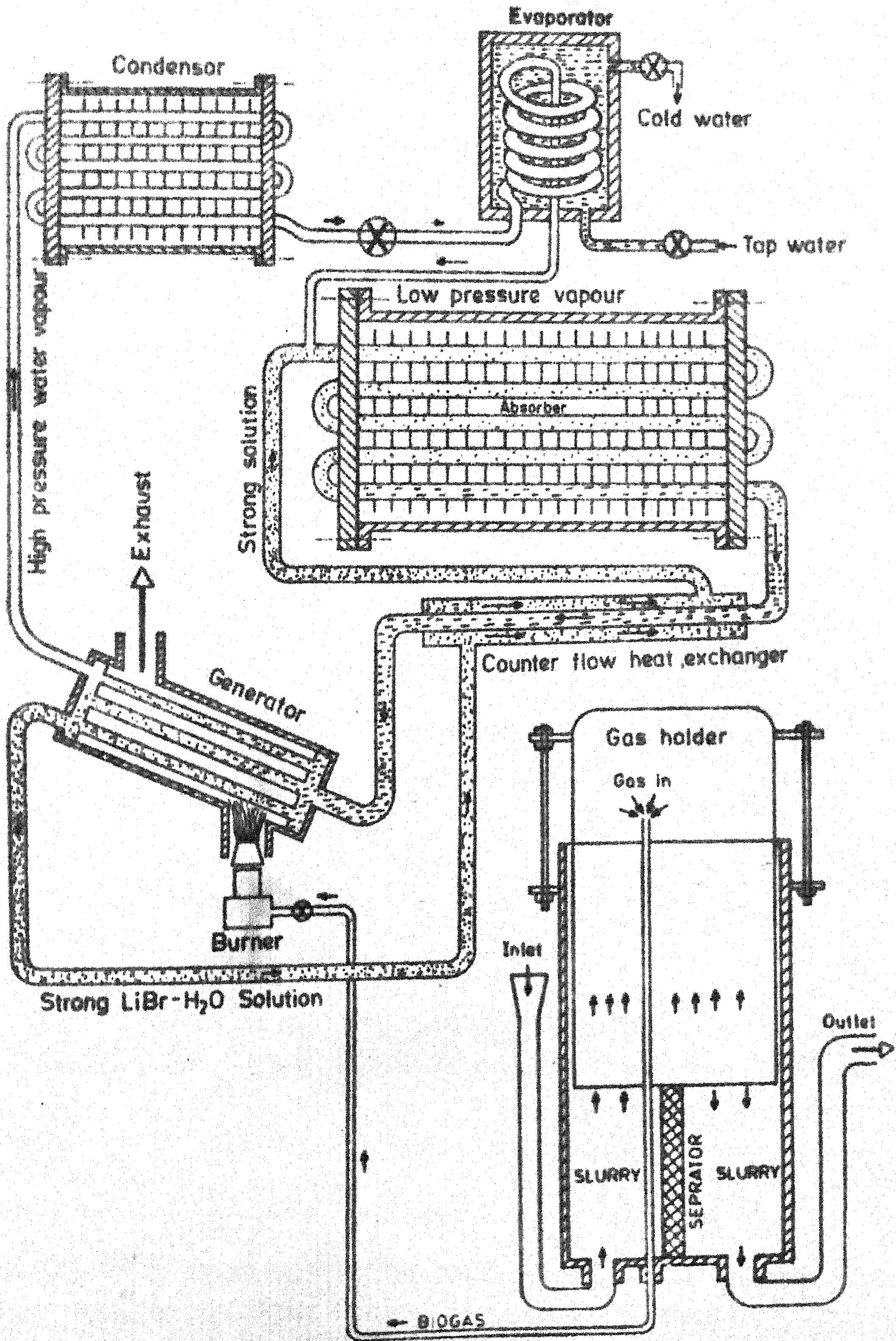

Fig. 4.3 Schematic view of the experimental set-up

Fig. 4.4 Experimental set-up

Fig. 4.5 View of Gobar-Gas Plant

CHAPTER - V

RESULTS AND DISCUSSION

5.1 Analytical Results

COP (for P_g = 40, 50, 60, 70 and 80 mm of Hg and HE effectiveness, $\varepsilon = 0.75$) and Q_{gas} with T_g are shown in Fig. (2.2) having concentration below 70%. Evidently the variation in COP with T_g is more dominant than the biogas energy, Q_{gas}.

The cost of biogas was computed for p_g = 40, 50, 60, 70 and 80 mm of Hg having HE effectivenesses of 0.65, 0.75 and 0.85 for 0.7, 1.4 and 2.1 kW of cooling capacities. The life of the biogas plant was assumed as 15 years having 10% interest rate. Analysis of the system has been carried out with precooler (PC), ε_1 and preheater (PH), ε_2 both (i.e., $\varepsilon_1 = \varepsilon_2 = \varepsilon$) and without precooler (i.e., $\varepsilon_1 = 0$, using PH only). Figures (5.1 to 5.5) exhibit variation in cost with generator temperature for a given generator pressure and evaporator temperature for different tonnages.

(i) Variation in cost with pressure

The cost variation with T_g for different pressures (p_g) show that the system operating at higher pressures are costlier than that at lower pressures. With the difference of 10 mm of Hg between two pressures, the cost variation is about 1.3%.

(ii) Variation in cost with TR

Cost variation for a fixed generator pressure and effectiveness differs significantly for all values of TR Figs.(5.1 to 5.4)whereas, the T_{go} values for all TR are same as is evident from Eq. (2.33).

Figures(5.6 and 5.7) represent the optimum generator temperature and cost of biogas for various values of parameters.

(iii) Variation in cost with HE effectiveness

For decrease in effectiveness for about 10% the cost increases for about 2% under optimum operating conditions. It shows a linear variation in cost with change in effectiveness within ranges of our study.

Analysis have been carried out for:

(a) using precooler and preheater both (i.e., $\epsilon_1 = \epsilon_2 = \epsilon$)

(b) with preheater only (i.e., $\epsilon_1 = 0$)

The results for these two cases are shown in Fig. (5.8).

It is seen that the latter is costlier (about 1.5 to 2%) than the former. But the latter is generally allowed in small units in view of simplicity.

The multiplier shown in Fig. (5.9) can be used to determine T_{go} for evaporator temperatures other than 5°C. To do this one should get T_{go} from Figures (5.1 to 5.5) for a set of operating variables and evaporator temperature of 5°C. Then this T_{go} is multiplied by the multiplier to get the required value.

5.2 Experimental Set-up

The system components have been fabricated and assembled. The absorber is kept at about 80 cm above the generator. Inclined Hg-manometers are used to measure the generator and evaporator pressures. Water manometer and wet-test meter are used to get the pressure and the flow rate of the biogas, respectively. Most of the joints are brazed. Only the polythene tube connections to the absorber are clamped and sealed using epoxy. The system has been evacuated to 1 atmosphere. The experiment was not possible due to some minor leakages. After a few months of trial it has been realized that it would take longer time which became a contraint in the present time bound programme.

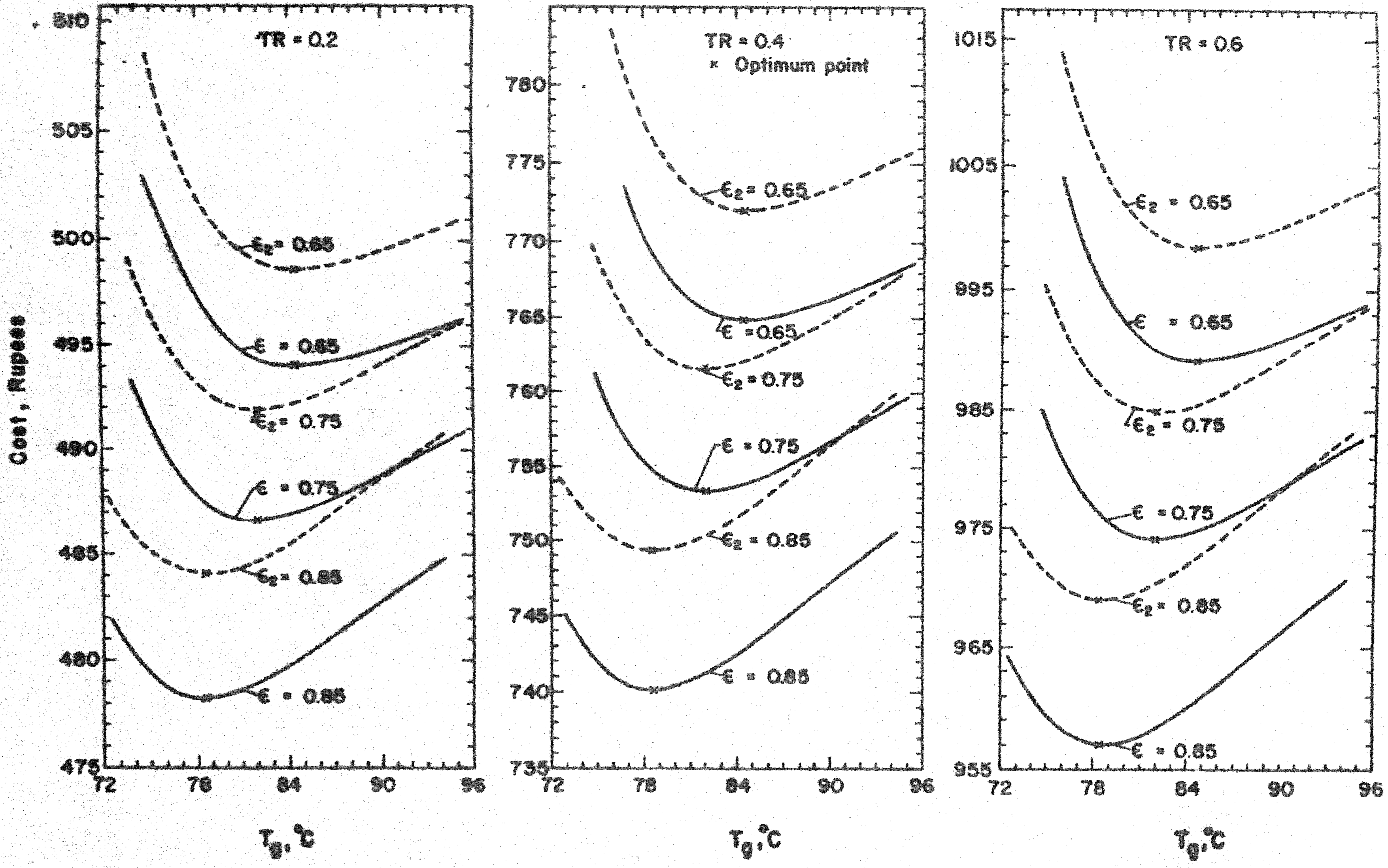

Fig.5.1 Variation in cost with generator temperature (T_g) for different tonnages (TR) and HE effectiveness (P_g = 40 mm of mercury and T_e = 5 °C).

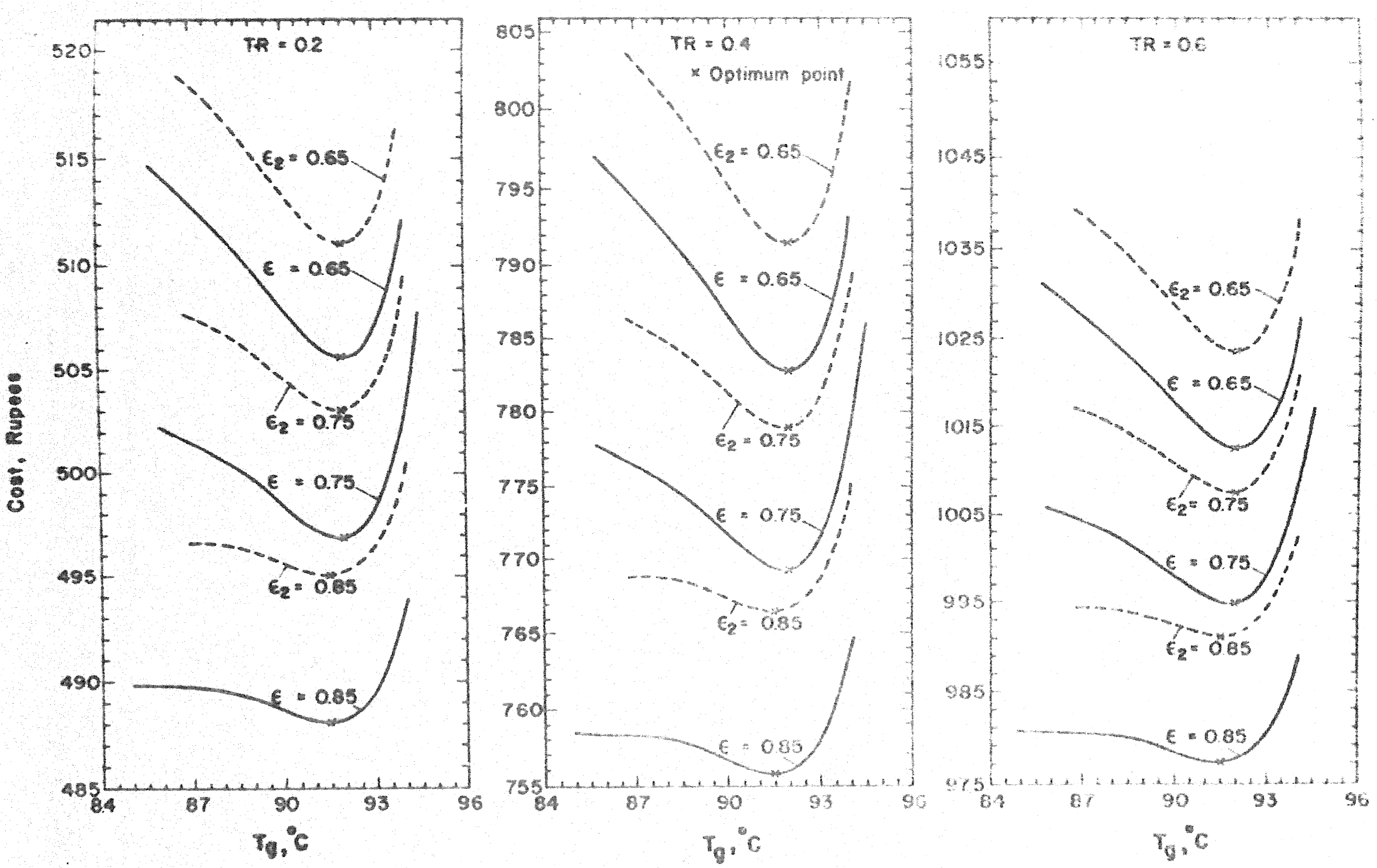

Fig.5.2 Variation in cost with generator temperature (T_g) for different tonnages (TR) and (HE) effectiveness (P_g = 50 mm of mercury and T_e = 5 °C)

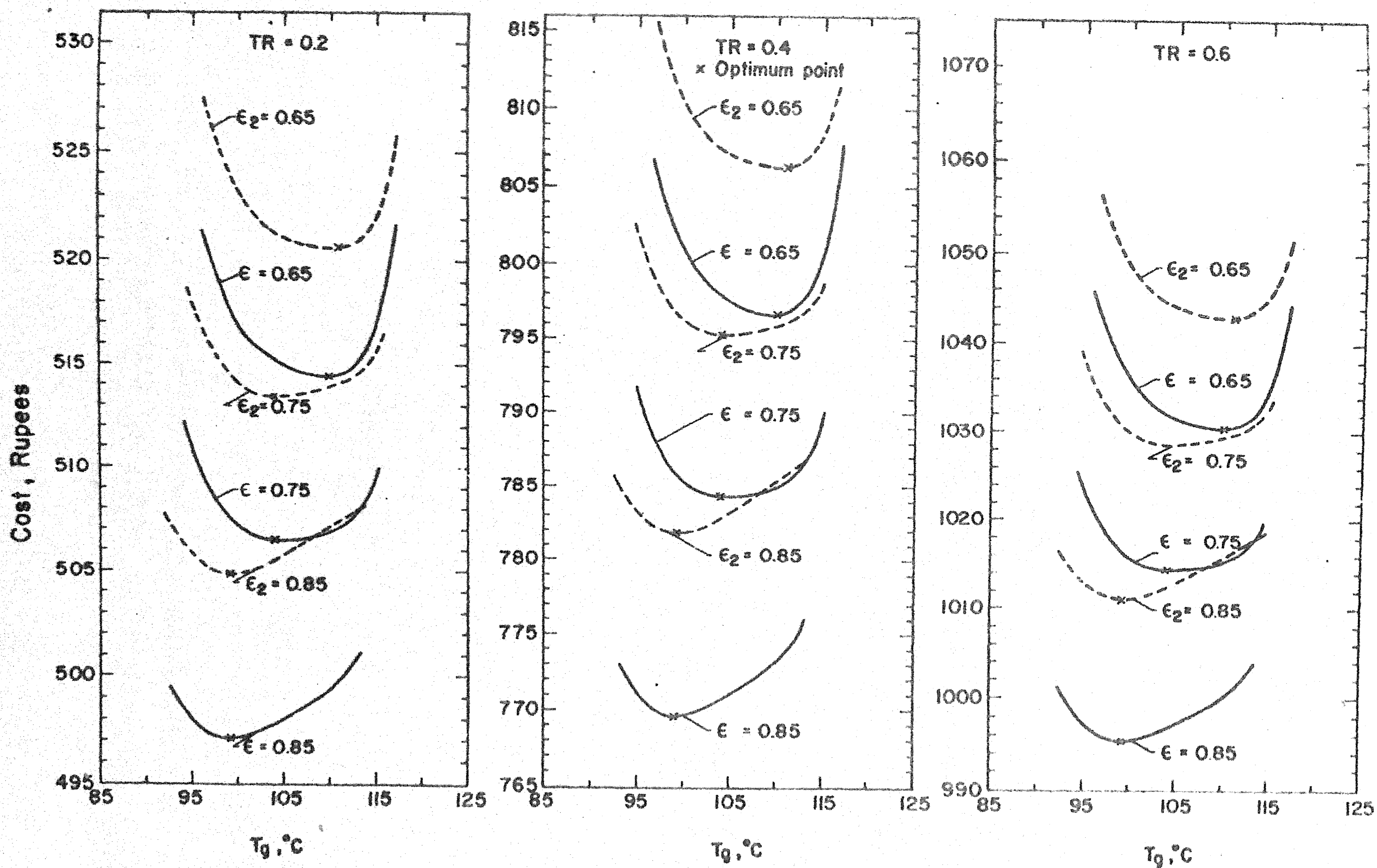

Fig.5.3 Variation in cost with generator temperature T_g, for different tonnages (TR) and HE diffectivnesses (p_g = 60 mm of mercury and T_e = 5 °C).

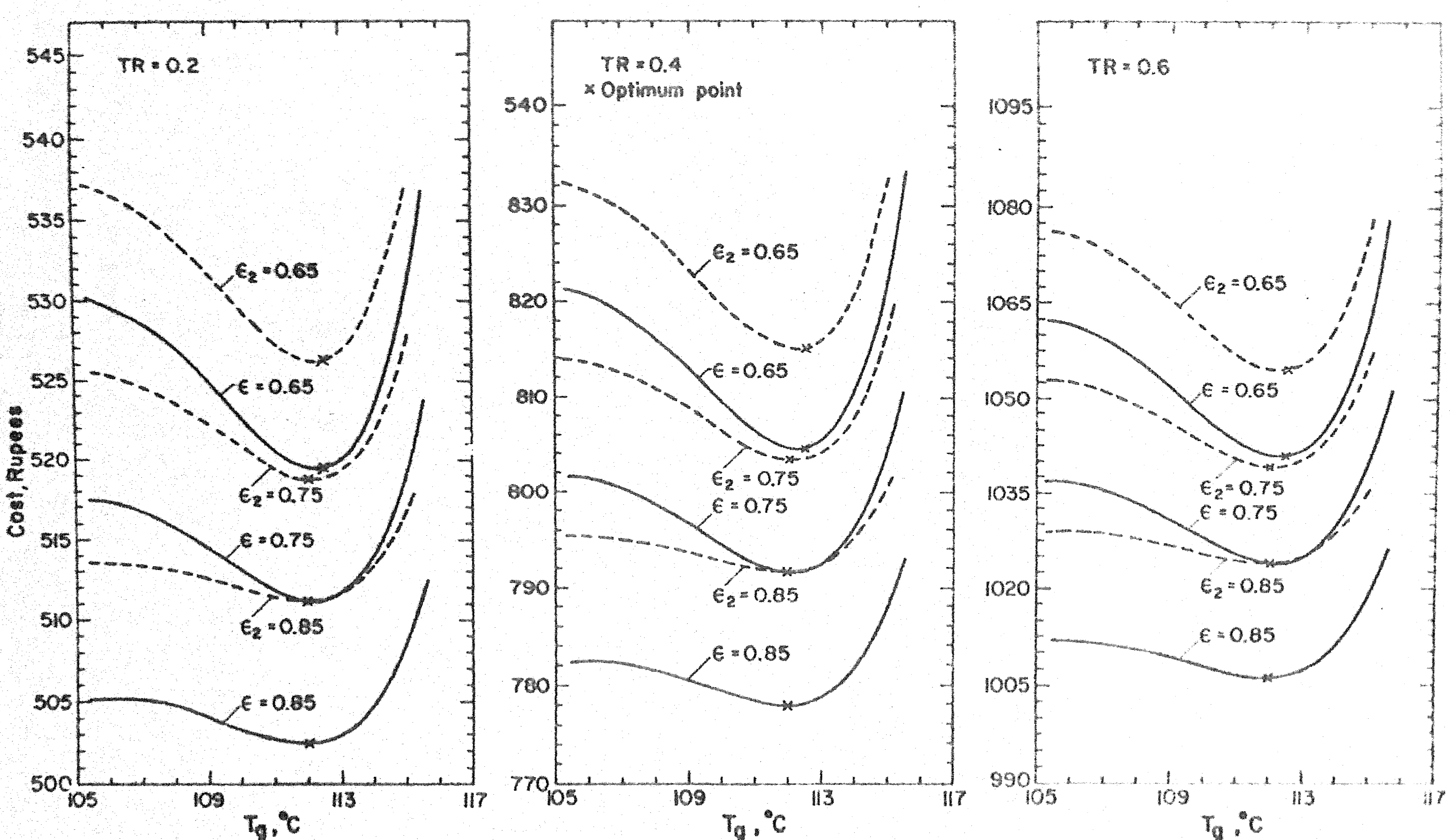

Fig.5.4 Variation in cost with generator temperature T_g, for different tonnages (TR) and HE effectiveness (p_g = 70 mm of mercury and T_e = 5°C)

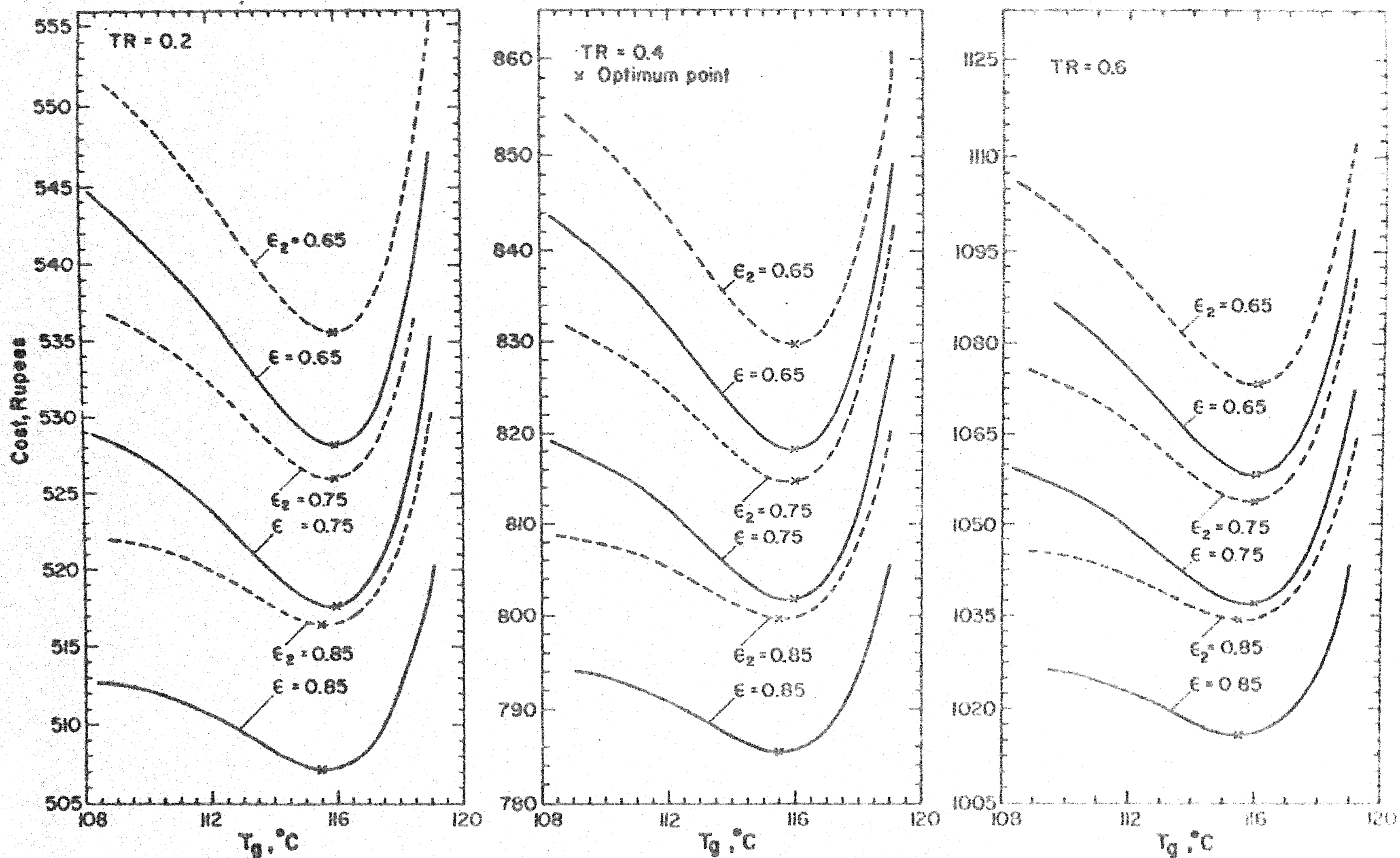

Fig.5.5 Variation in cost with generator temperature T_g, for different tonnages (TR) and HE effectivenesses (p_g = 80 mm of mercury and T_e = 5°C)

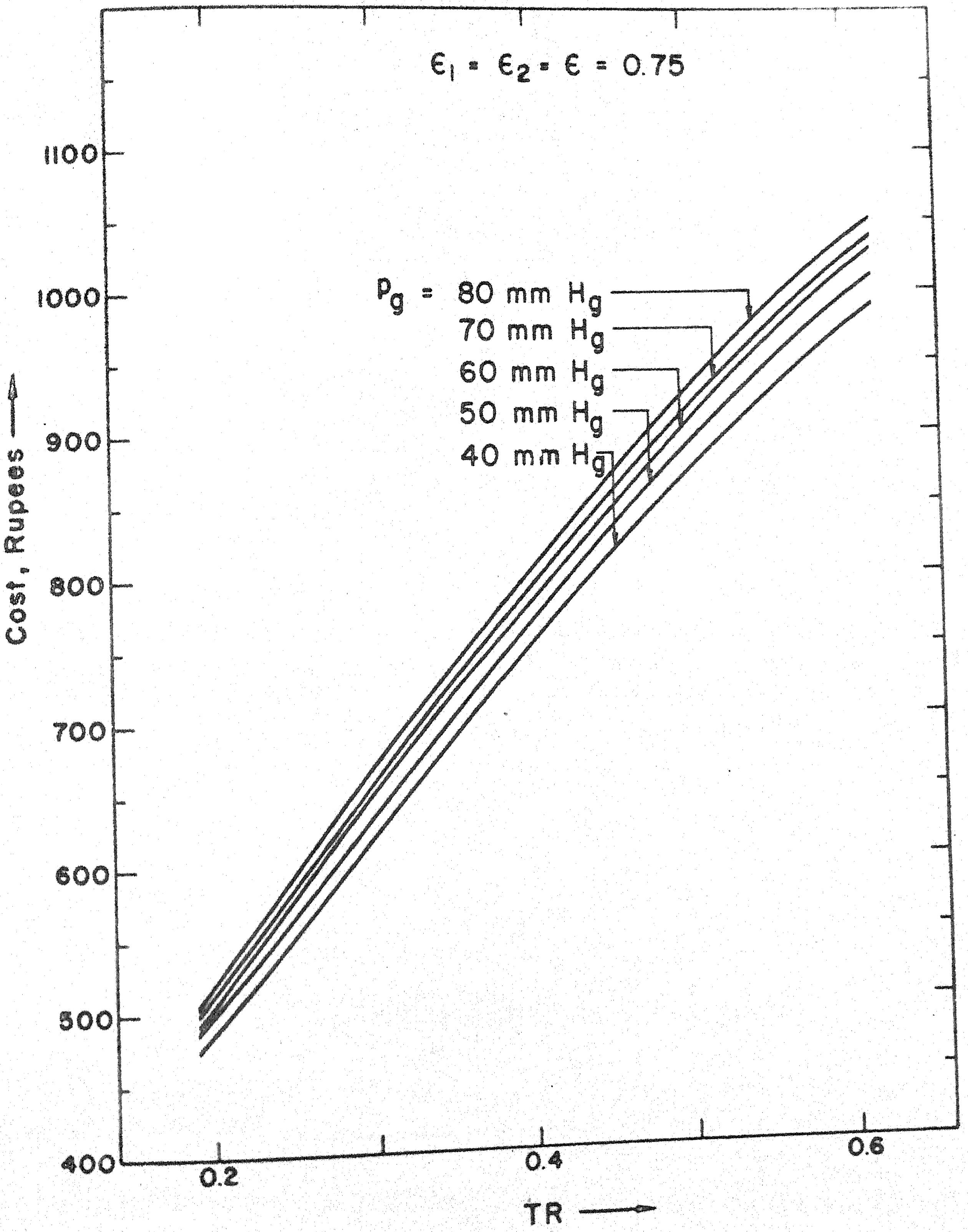

Fig.5.6 Variation in cost with TR for different generator pressures p_g.

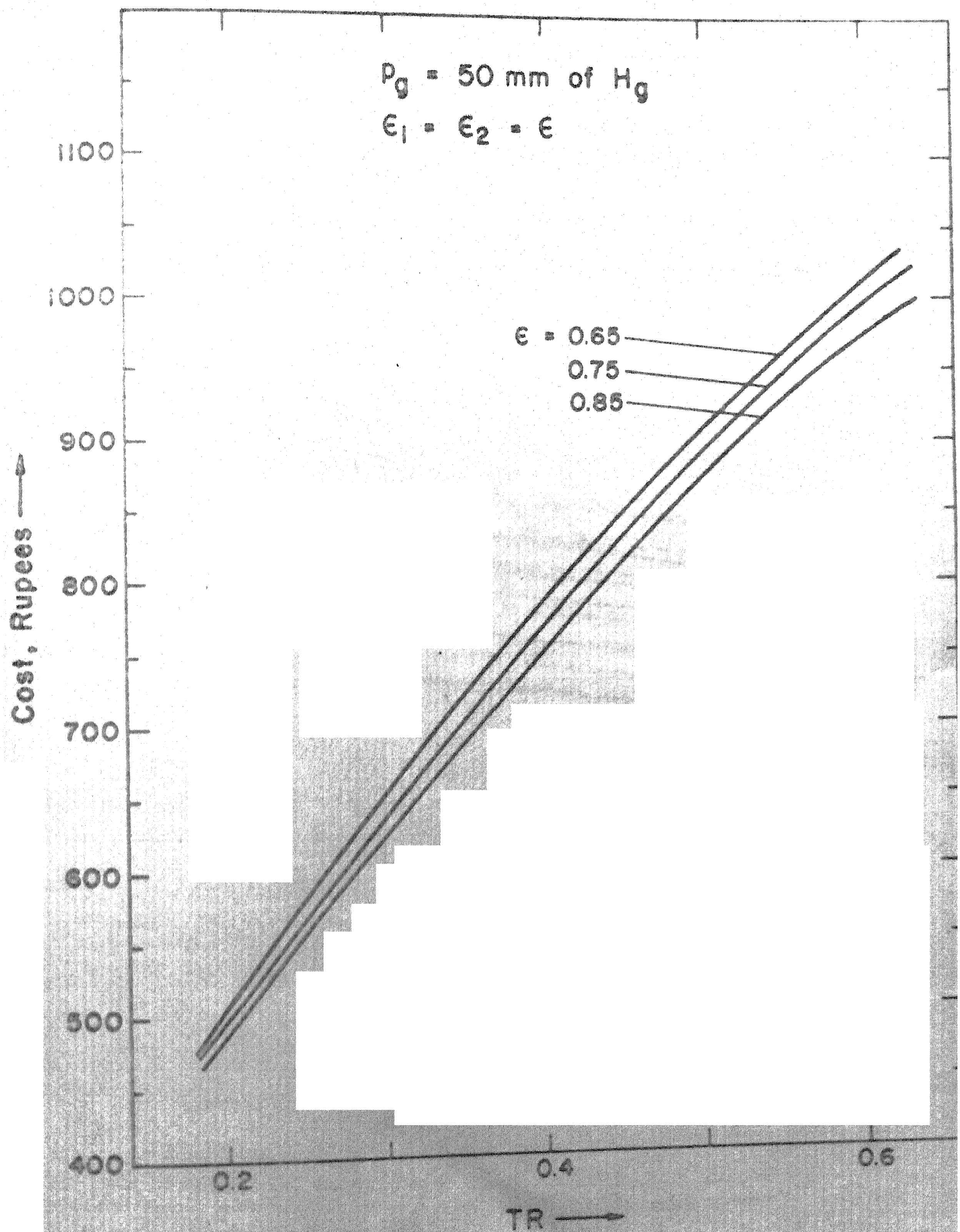

Fig.5.7 Variation in cost with TR for different HE effectiveness.

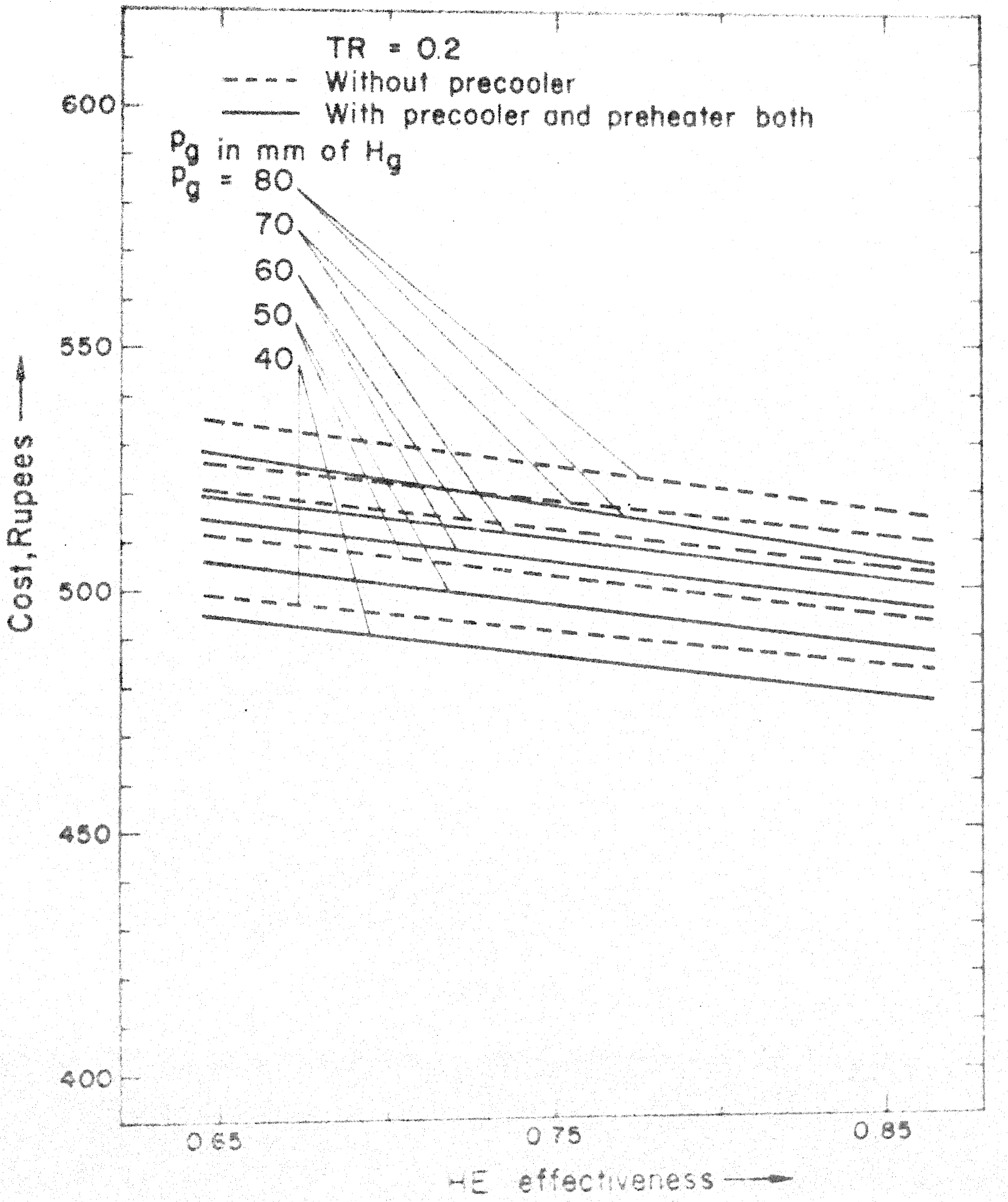

Fig. 5.8 Variation in cost with HE effectiveness for differen[t] generator pressures p_g.

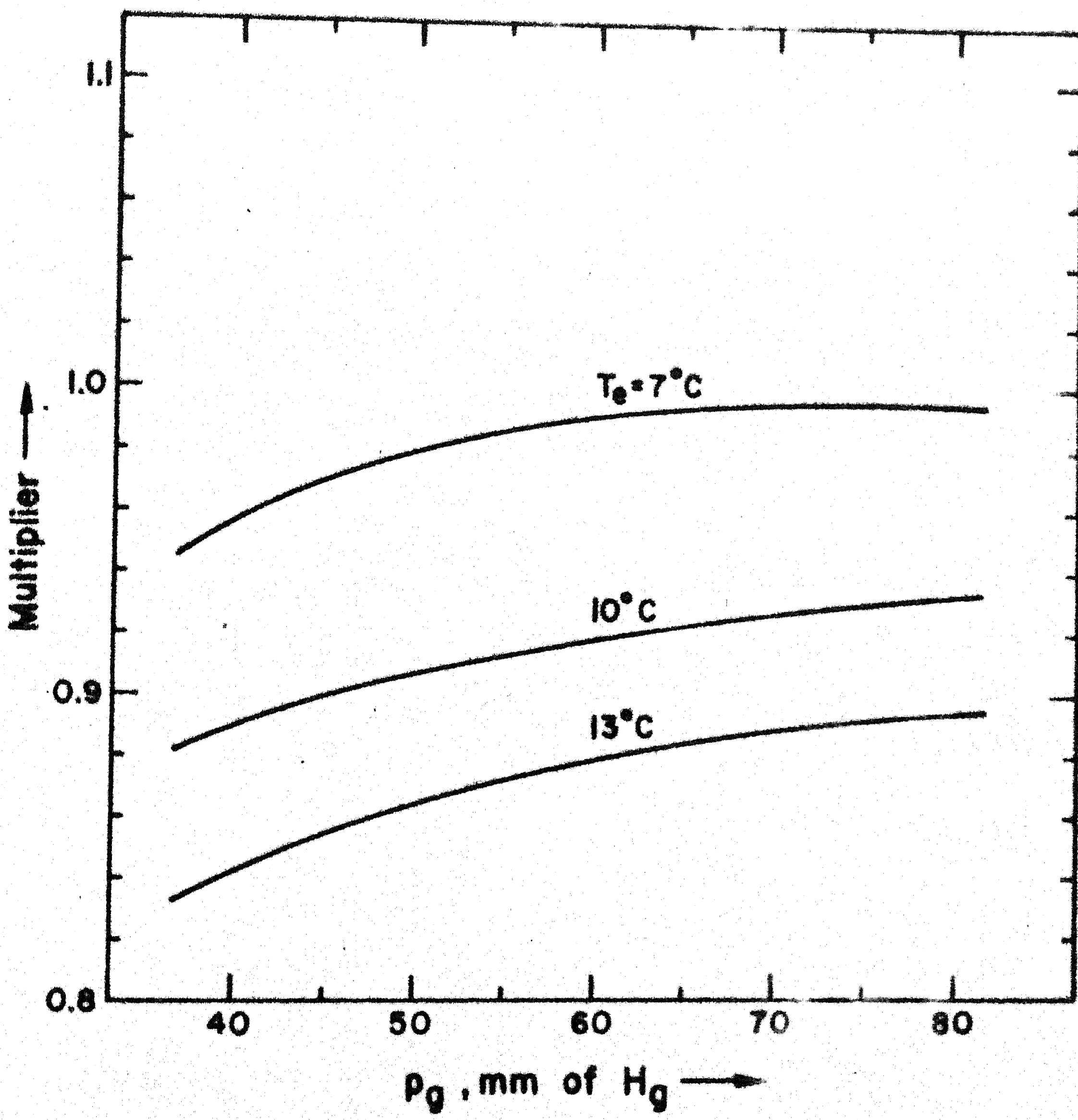

Fig.5.9 Multiplier for optimum generator temperature

The biogas plant was fed with 250 kg of slurry (equal weight of gobar + water) upto 0.23 m^3 volume of the drum initially. The recharging was started after 22 days of the initial charge, and was continued with 10 kg of slurry. The biogas generated from the plant was available at about 200 mm water head when heat was applied to the digester cylinder. Under normal winter temperature, the pressure of the biogas has been measured to be 100 mm of water.

CHAPTER - VI

CONCLUSION

1. The optimum generator temperature has been computed for the LiBr-H_2O absorption system using biogas energy for a wide range of operating conditions.

2. The biogas cost goes up by 1.3% for every 10 mm of rise in the generator pressure.

3. The optimum cost of the biogas for the system goes up by about 2% for every 10% decrease in effectivenesses of heat exchangers.

4. The cost of biogas goes up by 1.5 to 2% if the system operates without a precooler.

5. The multipliers have been presented for utilization of the present optimum results for evaporator temperatures other than 5°C.

6. To facilitate the user the optimum values of generator temperature are presented using capacity of refrigeration system as a variable for different operating variable.

7. The procedure is developed for design of various components of the vapour-absorption system.

8. After fabrication of all designed components, the system has been assembled for experimental purpose. The provisions are made for adjustment of relative elevation between the generator and absorber. This enables us to conduct experiment at other operating conditions as well.

9. The biogas was generated and is ready for the use in the system.

10. Components for this refrigeration system when fabricated and assembled in the laboratory has the problem of leakage. This is more so because it has to operate at low pressures which is possible only if the system is completely evacuated. The leakage problem becomes more acute because, in order to instrument the system, number of gauges and temperature transducers had to be inserted at several points. Making it leakage free is one of the most time consuming job. The leakage will not be a problem if the sealing etc. is done more professionally.

REFERENCES

1. Grover, P.D., Utili..ation of Agricultural, Forest and Industrial Wastes Through Renewable Biomass Energy Brequetted Fuel, at all India seminar on alternative energy sources - their applications and constraints on 19th and 20th March, 1983.

2. Murthy, V.S., Biogas Plans in Gujrat, same as [1]

3. Gupta, B.D., Feasibility of Biogas as Alternative Energy Source, same as [1]

4. Gupta, Gopal, Constraints in Using Family Size Biogas Plants and Their Remedies, same as [1]

5. Gujral, G.S. and Vasudevan, P., Utilization of Wasteland Biomass Socchrarum Munja (Sorkanda), same as [1]

6. Ghate, P.B. and Singh, K.K., Action Research in Biogas Development, Seminar on Biogas Production Technology, Sept. 27-30, 1970, Organised by Directorate of Extension, Ministry of Agriculture and Irrigation, New Delhi.

7. Prasad, M., Optimum Generator Temperature for LiBr-Water Absorption System, I.I.F. - I.I.R. - Commissions B_1, B_2, E_1, E_2, Mons (Belgium), 1980.

8. Janta Gobar Gas Plant, Gobar Gas Research Station, Ajitmal, Etawah, India, (by personal contact to KVIC, Kalyanpur, Kanpur).

9. Infant Ferreira, C.A., Thermodynamic and Physical Property Data Equations for Ammonia - Lithium Nitrate and Ammonia Sodium Thiocyanate Solutions, Solar Energy, Pergaman Press Ltd., Great Britain, Vol. 32, No. 2, 1984, pp. 231-236.

10. Mansoor, A. and Patel, V., Thermodynamic Basis for the Choice Working Fluids for Solar Absorption Cooling Systems, Solar Energy, 22, 1979, pp. 483-491.

11. Prasad, M., Kaul, P.N. and Agrawal, H.C., Solar Powered Air Conditioning System, 'All India Seminar on Solar Energy Prospects and Problems', 2-3 Jan. 1981.

12. Renz, M. and Steimle, F., Comparison of Thermodynamic Properties of Working Fluids For Absorption System, IIR, Commissions $E_1 - E_2$, Jerusalem (Israel), 1982-83, pp. 61-67.

13. Prasad, M. and Gupta, V.K., Optimum Generator Temperature for Solar Powered Absorption System, Solar Energy Symposium, Baghdad, Iraq, 1981.

14. Ashrae Handbook, 1981, Fundamentals.

15. Sofrata, H., Nasser, A., Khoshaim, B. and Megahed, M., Computer Package for the Design and Optimization of Absorption Air Conditioning System Operated by Solar Energy, Alternative Energy Sources, V.2, ed. T.N. Veziroglu, 1983, pp. 221-232.

16. K.A. Nagabushana, Computer Aided Design of Cooling Tower, M. Tech. Thesis, Aug. 1983, I.I.T.,Kanpur.

17. Kadambi, V. and Prasad, M., An Introduction to Energy Conversion, (Vol. II, Energy Conversion Cycles), Wiley Eastern Limited, 1974, pp. 39-40.

18. Donald, L. Wise, Fuel Gas Production From Biomass, Vols. I and II CRC Press Inc., Boca Raton, 1981, pp. 53-71.

19. Prasad, M., Refrigeration and Air Conditioning, Wiley Eastern Limited, 1983, pp. 345-355.

20. Dossat, R.J., Principles of Refrigeration, Wiley Eastern Ltd., 2nd Edition, SI Version pp. 177-228.

21. Ashrae Guide And Data Book, 1965, pp. 977-982.

22. Chato, J.C., Journal of American Society of Refrig. Air Conditioning Engg., Feb. 1962, p. 52.

23. Kern, D.Q., Process Heat Transfer, McGraw Hill, 1950, Ist. Ed., New York, pp. 201-220.

24. Kothandaraman, C.P., and Subramanyam, S., Heat And Mass Transfer Data Book, Wiley Eastern Ltd., 1977, 3rd Ed., pp. 13-16.

25. Jacob, M., Heat Transfer, John Wiley and Sons Inc., New York, 1949 and 1957, Vols. I and II.

26. Mc Adams, W.H., Heat Transmission, McGraw Hill Book Co., Inc., New York, 1954, 3rd Ed.

27. Holman, J.P., Heat Transfer, McGraw Hill International Book Co., 1981, 5th Ed., p. 285, pp. 292-295.

28. Threlkeld, J.L., Thermal Environmental Engg., Printice-Hall Inc., 1962, pp.234-271.

29. Zabronsky, H., Temperature Distribution and Efficiency of a Heat Exchanger Using Square Fins on Round Tubes, ASME Transactions, Journal of Applied Mechanics, Dec. 1955, Vol. 77, p. 119.

30. Carrier, W.H., and Anderson, S.W., The Resistance to Heat Flow Through Finned Tubing (Heating, Piping, and Air-Conditioning, May 1944, p. 304).

31. Bogart, Marcel, Ammonia Absorption Refrigeration in Industrial Processes, Gulf Publishing Co. Book Div., 1981. pp. 119-122.

32. Sixteenth International Congress of Paris, 1933, p. 210, Commissions C2, IIR, Paris.
Alloush, A., and Gosney, W.B., Thermal Conductivity of Some Salts Solutions by Transient Hot Wire Method, 16th International Congress of Refrigeration, Commissions B1, Paris, 1933, pp. 208-213.

33. Collier, J.G., Convective Boiling and Condensation, McGraw Hill Book Co., Ltd. (U.K.), 1972, pp.139-141, pp. 11-14, pp. 123-124.

34. Prasad, M., Two Phase Analysis to Condensation in Helical Coil Heat Exchanger, Proceedings of 11th National Conference on Fluid Mechanics and Fluid Power, B.H.E.L. (R and D), Hyderabad, 16-18 Dec., 1982, pp. 37.41.

35. Rohsenow, W.M., A Method of Correlating Heat Transfer Data for Surface Boiling of Liquids, Trans. ASME, 74, 1952, pp. 969 - 975.

36. Adams, J.A., Rogers, D.F., Computer Aided Heat Transfer Analysis, McGraw Hill Inc., 1973, pp.6-54.

37. Brown, C.K., Gawvin, W.H., Combined Free and Forced Convection, I, II, Can. J. of Chem. Engg., Vol. 43, No. 6, 1965, pp. 306-313.

APPENDIX - A

Thermodynamic Properties of the LiBr-H_2O Solution and Water

From standard references [14,16,32] the various properties are listed below:

Properties (i) to (ix) are in F.P.S. units (h, Btu/lb, T. °F and P. psia).

(i) Solution temperature : $T = AT' + B$

(ii) Refrigerant temperature : $T' = (T - B)/A$

(iii) $A = -2.00755 + 0.16976\,x - (3.133362\,E - 3)\,x^2 + (1.97668\,E - 5)\,x^3$

(iv) $B = 321.128 - 19.322\,x + 0.374382\,x^2 - (2.0637\,E - 3)\,x^3$

(v) Vapour pressure : $\log_{10} P = C + D/(T' + 459.72)$
$E/\,(T' + 459.72)^2$

where,

$C = 6.21147$ $\qquad 0 \geq T' \leq 230$ °F

$D = -2886.373$ $\qquad 40 \geq T \leq 350$ °C

$E = -337269.46$ $\qquad 45\% \geq x \leq 70\%$

(vi) Enthalpy of the solution: $h = A_1 + A_2T + A_3T^2$

(vii) $A_1 = -1015.07 + 79.5387\,x - 2.358016\,x^2 + 0.03031583\,x^3 - (1.400261\,E - 4)\,x^4$

(viii) $A_2 = 4.68108 - (3.037766\,E - 1)\,x + (8.44845\,E - 3)x^2 - (1.047721\,E - 4)\,x^3 + (4.80097\,E - 7)x^4$

(ix) $A_3 = -(4.9107\ E-3) + (3.83184\ E-4)\ x$
$- (1.073963\ E-5)\ x^2 + (1.3152\ E-7)\ x^3$
$- (5.897\ E-10)\ x^4$

T = Solution temperature, °F, having range 60°F $\geq$ T $\leq$ 330°F

x = LiBr concentration, percent, having range 40% $\geq x \leq$ 70%

The properties listed below are in S.I. units (h, kJ/kg; C_p, kJ/kg; T, °C)

(x) Specific heat of LiBr-water solution:

$$C_{p_L} = 4.259 - 0.053343\ x + (2.307\ E-4)x^2$$

(xi) Enthalpy of saturated water:

$$h_f = (0.99615\ T + (1.8239\ E-6)T^2 - 0.13468 * (10 ** (-0.036\ T)) + 0.13468) * 4.187$$

(xii) Enthalpy of saturated vapour:

$$h_g = H_{fg} + h_f$$

(xiii) Latent heat of vaporization:

$$h_{fg} = (597.34 - 0.555\ T - 0.2389 * (10 ** (5.1463 - 1540/(T + 273.15)))) * 4.187$$

(xiv) Enthalpy of superheated vapour:

$$h_{s\rho} = 1.925 * T_g - 0.126\ T_c + 2500$$

(xv) Specific heat of water:

$$C_{pw} = 4.2097187 - (1.4125\ E-3)\ T + (1.375\ E-5)T^2$$

APPENDIX - B

COMPUTER RESULTS FOR OPTIMISATION OF GENERATOR TEMPERATURE TG

CALCULATION OF PROPERTY VALUES AT GENERATOR TEMPERATURE PG=80 MM OF MERCURY

```
TC  =  47.078   TA=  47.078    TE= 5.00004  X1=61.38680
H1  = 135.785   H6=2510.082    H6D=2510.082 H4= 196.926
H4D= 196.926    E1=   0.000    E2 =  0.750  PG= 80.000
```

S.NO.	TG	X	H7	H7D	H2D	H3	COP
1	100.605	63.000	244.860	146.124	208.941	2687.733	0.60151
2	102.363	63.700	251.279	150.363	209.724	2691.117	0.64538
3	104.151	64.400	257.800	154.692	210.499	2694.559	0.67092
4	105.970	65.100	264.413	159.093	211.270	2698.060	0.68734
5	107.819	65.800	271.107	163.547	212.045	2701.619	0.69860
6	109.699	66.500	277.871	168.034	212.829	2705.238	0.70668
7	111.610	67.200	284.694	172.533	213.629	2708.917	0.71268
8	113.552	67.900	291.565	177.021	214.453	2712.656	0.71726
9	115.527	68.600	298.474	181.474	215.308	2716.457	0.72085
10	117.533	69.300	305.409	185.867	216.204	2720.319	0.72374

CALCULATION OF COEFFICIENTS OF EQ.(2.16)

```
A0=   0.740998E+01          A1=  -0.112002E+00
A2=  -0.269506E-02          A3=   0.676124E-04
A4=  -0.537664E-06          A5=   0.852616E-09
A6=   0.493741E-10          A7=  -0.662301E-12
A8=   0.282842E-14          A9=  -0.246315E-17
```

Err %age	TG	COP
1.153035	100.604900	0.601506
0.871504	102.362980	0.645381
0.765508	104.151100	0.670923
0.175221	105.969570	0.687345
0.305632	107.818640	0.698603
0.460939	109.698610	0.706680
0.280163	111.609740	0.712678
0.085440	113.552310	0.717261
0.320410	115.526620	0.720853
0.075189	117.532920	0.723738

VALUES CORRESPONDING TO OPTIMUM GENERATOR TEMPERATURE TG

COP= 0.727325   QGAS=15412.98   TG=116.

V	CT	TR	C1	C2
3.776	526.0250	0.2	4082.2	455.163
7.553	814.7799	0.4	6659.3	664.822
11.329	1053.9344	0.6	8865.5	829.763

87602